Inorganic Chemistry

Article

pubs.acs.org/IC

Amidinatogermylene Derivatives of Ruthenium Carbonyl: New Insights into the Reactivity of $[Ru_3(CO)_{12}]$ with Two-Electron-Donor Reagents of High Basicity

Lucía Álvarez-Rodríguez,[†] Javier A. Cabeza,*[,†] Pablo García-Álvarez,*[,†] Enrique Pérez-Carreño,[‡] and Diego Polo[†]

[†]Departamento de Química Orgánica e Inorgánica-IUQOEM, Universidad de Oviedo-CSIC, E-33071 Oviedo, Spain

[‡]Departamento de Química Física y Analítica, Universidad de Oviedo, E-33071 Oviedo, Spain

Supporting Information

ABSTRACT: The reactivity of ruthenium carbonyl with amidinatogermylenes of the type Ge(R_2bzam)^{t}Bu (R_2bzam = *N*,*N*′-disubstituted benzamidinate) was studied for R = ^{t}Bu ($\mathbf{1_{tBu}}$) and ^{i}Pr ($\mathbf{1_{iPr}}$). The mono-, bi-, and/or trinuclear derivatives $[Ru(\mathbf{1_R})(CO)_4]$, $[Ru(\mathbf{1_R})_2(CO)_3]$, $[Ru_2(\mathbf{1_{iPr}})(CO)_7]$, $[Ru_3(\mathbf{1_{tBu}})(CO)_{11}]$, $[Ru_3(\mathbf{1_{tBu}})_2(CO)_{10}]$, and $[Ru_3(\mathbf{1_R})_3(CO)_9]$ (R = ^{t}Bu, ^{i}Pr) were isolated in yields that depend upon the reactant ratio and the reaction temperature. The experimental data are consistent with the proposal that, at room temperature, the trinuclear complexes $[Ru_3(CO)_{12}]$, $[Ru_3(\mathbf{1_R})(CO)_{11}]$, and $[Ru_3(\mathbf{1_R})_2(CO)_{10}]$ form an adduct with the germylene $\mathbf{1_R}$ that may evolve through two different reaction pathways, (a) releasing a CO ligand (thus leading to the corresponding trinuclear CO-substituted product) and/or (b) cleaving the cluster framework (thus leading to mononuclear germylene-containing products). At 90 °C, additional processes are also possible, such as the reactions of $\mathbf{1_R}$ with $[Ru(\mathbf{1_R})(CO)_4]$ or $[Ru_3(\mathbf{1_R})_3(CO)_9]$, which both give $[Ru(\mathbf{1_R})_2(CO)_3]$, or the reactions of $[Ru(\mathbf{1_{tBu}})(CO)_4]$ and $[Ru(\mathbf{1_{iPr}})(CO)_4]$ with $[Ru_3(CO)_{12}]$, which give $[Ru_3(\mathbf{1_{tBu}})(CO)_{11}]$ and $[Ru_2(\mathbf{1_{iPr}})(CO)_7]$, respectively. This wide reaction panorama helps rationalize previously reported outcomes of reactions of $[Ru_3(CO)_{12}]$ with other reagents of high basicity, such as trialkylphosphines or N-heterocyclic carbenes, including results for which no satisfactory explanation has been hitherto provided.

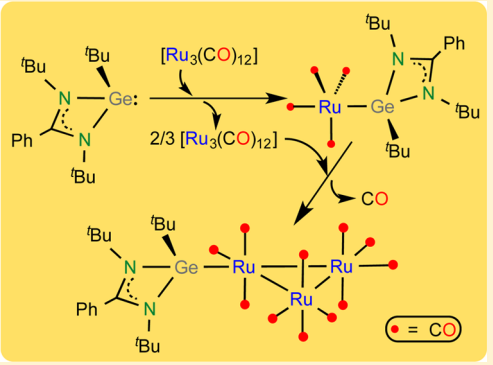

INTRODUCTION

The most common ruthenium carbonyl, $[Ru_3(CO)_{12}]$, is a fundamental reagent of key importance for the synthesis of a great variety of carbonyl ruthenium complexes. Its reactions involve, in many cases, CO-substitution processes. In this context, it is well-known that common two-electron-donor reagents (L), such as monodentate phosphines[1] (PR_3) or N-heterocyclic carbenes (NHCs),[2] may give one or various mono- and/or trinuclear ruthenium carbonyl derivatives (Scheme 1).

Many reactivity and kinetics studies involving PR_3 ligands (those with NHCs are much more scarce) have also shown that these reactions proceed through mechanisms that can be dissociative, associative, or a mixture of both and that the type of mechanism and the nature and ratio of the reaction products depend upon the ratio of the reactants, the reaction conditions (concentration and temperature), and the nature of the nucleophilic reagent.[1] In the case of reagents of high σ-basicity and/or weak π-acidity, such as trialkylphosphines[3] and NHCs,[4] the reactions are generally fast (occurring at room temperature), preferably associative, and lead to extensive cluster fragmentation at low $[Ru_3(CO)_{12}]$-to-reagent ratios. However, a general "how-and-why" explanation of these experimental results has not been hitherto provided. Therefore, given the current importance that $[Ru_3(CO)_{12}]$ has as a primary reagent, not only in inorganic synthesis but also in catalysis,[5] any new insight that could shed more light into the reaction pathways

Scheme 1. Possible Products of a Reaction of $[Ru_3(CO)_{12}]$ with a Two-Electron-Donor Reagent (L = PR_3, NHC) at Room or Moderate Temperature

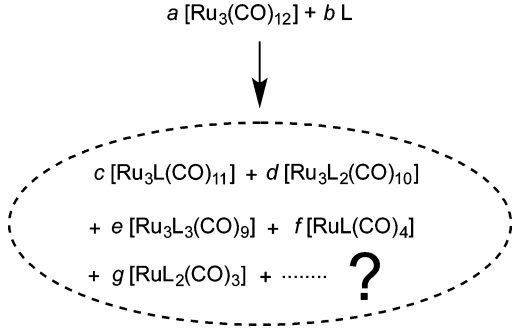

Received: January 12, 2015
Published: February 25, 2015

DOI: 10.1021/acs.inorgchem.5b00084
Inorg. Chem. 2015, 54, 2983−2994

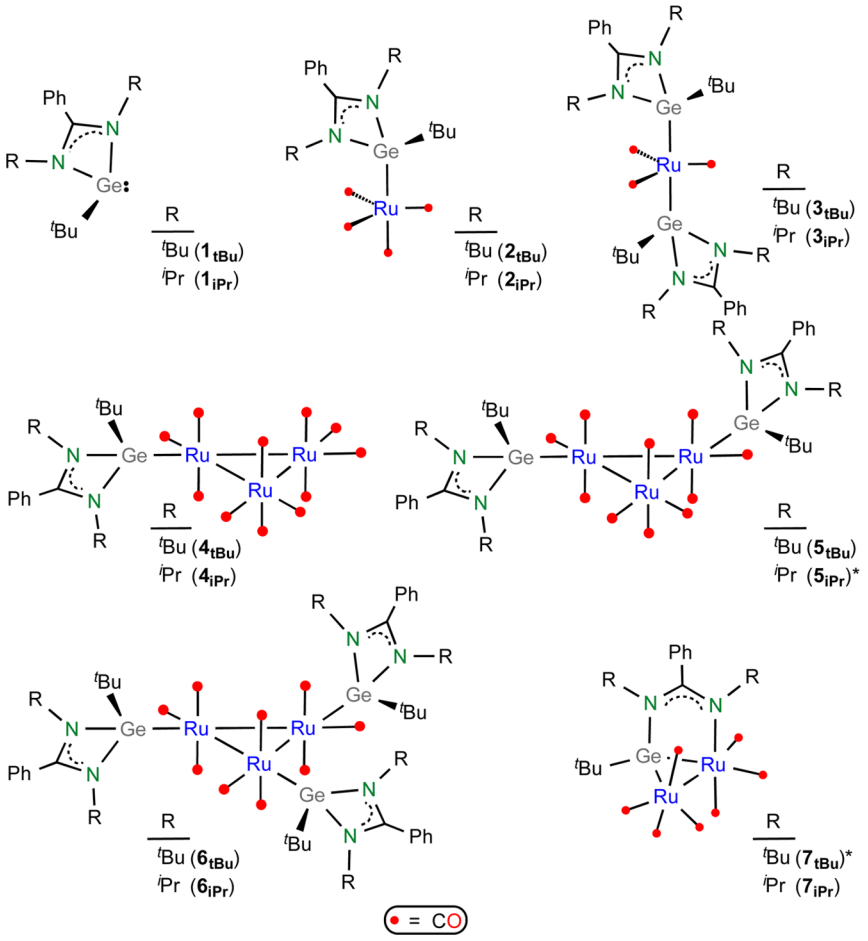

Figure 1. Schematic structures and abbreviated names of the germylenes used in this work and their reaction products. Those marked with an asterisk were not isolated or detected in the reaction mixtures.

pertinent to its reactions with two-electron-donor reagents would be greatly appreciated.

The past few years have witnessed an exponential growth of the chemistry of heavier tetrylenes (HTs).[6−10] Among the currently known HTs, those stabilized by an amidinate group have played a role of utmost importance in the development of the coordination chemistry of these two-electron-donor ligands,[8,9] since almost all of the elements of the transition metal (TM) series are nowadays known to form amidinato-HT−TM derivatives.[9] Some of these complexes have already been successfully tested as catalyst precursors for useful reactions in organic synthesis.[9a−e,10]

Continuing with our investigations on the coordination chemistry of HTs[11−14] and, in particular, on the reactivity of amidinatogermylenes with TM carbonyls,[11a,12−14] we now report that a study of the reactions of $[Ru_3(CO)_{12}]$ with benzamidinatogermylenes of the type Ge(R_2bzam)^{t}Bu (R_2bzam = *N*,*N*′-disubstituted benzamidinate) under different reaction conditions has allowed us to observe more reaction intermediates, products, and connections between them than those previously described for reactions of $[Ru_3(CO)_{12}]$ with other two-elecron-donor ligands. We also demonstrate herein that this wide reaction panorama can be used as a general tool that helps rationalize the outcomes of reactions of $[Ru_3(CO)_{12}]$ with other reagents of high basicity, such as trialkylphosphines or NHCs, including results for which no satisfactory explanation has been hitherto provided.

RESULTS

The schematic structures of the two amidinatogermylenes used in this work, namely, Ge(^{t}Bu$_2$bzam)^{t}Bu ($\mathbf{1}_{tBu}$) and Ge(^{i}Pr$_2$bzam)^{t}Bu ($\mathbf{1}_{iPr}$), and all of their (possible) ruthenium carbonyl derivatives (not all of these products were detected and/or isolated for both amidinatogermylenes) are depicted in Figure 1. Table 1 collects a summary of the reactions reported in this work, including the reaction conditions and the molar ratio of the reaction products containing germylene ligands (in some cases, the presence of $[Ru_3(CO)_{12}]$ among the reaction products was verified by IR spectroscopy, but its amount was not quantified).

Reactions Involving Ge(^{t}Bu$_2$bzam)^{t}Bu ($\mathbf{1}_{tBu}$). Ruthenium carbonyl reacted readily with 1 equiv of $\mathbf{1}_{tBu}$ at room temperature (Table 1, entry 1) to give a mixture of mononuclear ($\mathbf{2}_{tBu}$ and $\mathbf{3}_{tBu}$) and trinuclear derivatives ($\mathbf{4}_{tBu}$, $\mathbf{5}_{tBu}$, and $\mathbf{6}_{tBu}$) in which $\mathbf{2}_{tBu}$ was the major product. While all of $\mathbf{1}_{tBu}$ had reacted, some $[Ru_3(CO)_{12}]$ remained among the reaction products. Increasing the initial amount of $\mathbf{1}_{tBu}$ to 4 equiv (Table 1, entry 2) favored the formation of mononuclear $\mathbf{2}_{tBu}$ and $\mathbf{3}_{tBu}$ but decreased the amounts of trinuclear $\mathbf{4}_{tBu}$ and $\mathbf{5}_{tBu}$ down to undetectable levels, while the amount of $\mathbf{6}_{tBu}$ (relative to that of $\mathbf{2}_{tBu}$) did not change. A small amount of $[Ru_3(CO)_{12}]$ accompanied the reaction products.

As stated above, formation of mono- and/or trinuclear complexes of the types $[RuL_n(CO)_{5-n}]$ (n = 1, 2) and/or $[Ru_3L_n(CO)_{12-n}]$ (n = 1−3) have been previously observed in

DOI: 10.1021/acs.inorgchem.5b00084
Inorg. Chem. 2015, 54, 2983−2994

Table 1. A Selection of the Reactions Discussed in This Work[a]

No.	reactants	T, °C	t, h	[Ru($\mathbf{1}_R$)(CO)$_4$] ($\mathbf{2}_R$)[b]	[Ru($\mathbf{1}_R$)$_2$(CO)$_3$] ($\mathbf{3}_R$)[b]	[Ru$_3$($\mathbf{1}_R$)(CO)$_{11}$] ($\mathbf{4}_R$)[b]	[Ru$_3$($\mathbf{1}_R$)$_2$(CO)$_{10}$] ($\mathbf{5}_R$)[b]	[Ru$_3$($\mathbf{1}_R$)$_3$(CO)$_9$] ($\mathbf{6}_R$)[b]	[Ru$_2$($\mathbf{1}_R$)(CO)$_7$] ($\mathbf{7}_R$)[b]
				Reactions Involving $\mathbf{1}_{tBu}$					
1	[Ru$_3$(CO)$_{12}$] + $\mathbf{1}_{tBu}$	20	1	100[c]	10	7	10	4	0
2	[Ru$_3$(CO)$_{12}$] + 4 $\mathbf{1}_{tBu}$	20	1	100[c]	20	0	0	3	0
3	[Ru$_3$(CO)$_{12}$] + $\mathbf{1}_{tBu}$ + CO[d]	20	1	100[c]	0	0	0	0	0
4	$\mathbf{4}_{tBu}$ + CO[d]	20	2	0	0	100[c]	0	0	0
5	$\mathbf{4}_{tBu}$ + $\mathbf{1}_{tBu}$	20	1	100[c]	35	0	16	2	0
6	$\mathbf{4}_{tBu}$ + 3 $\mathbf{1}_{tBu}$	20	1	100	44	0	0	10	0
7	$\mathbf{5}_{tBu}$ + 4 $\mathbf{1}_{tBu}$	20	1	0	0	0	0	100	0
8	[Ru$_3$(CO)$_{12}$] + $\mathbf{1}_{tBu}$	90	2	0	0	100[c]	15	0	0
9	2/3 [Ru$_3$(CO)$_{12}$] + $\mathbf{2}_{tBu}$	90	2	0	0	100	0	0	0
10	[Ru$_3$(CO)$_{12}$] + 8 $\mathbf{1}_{tBu}$	100	3	0	100	0	0	0	0
11	$\mathbf{2}_{tBu}$ + 2 $\mathbf{1}_{tBu}$	100	3	0	100	0	0	0	0
12	$\mathbf{6}_{tBu}$ + 4 $\mathbf{1}_{tBu}$	100	3	0	100	0	0	0	0
13	$\mathbf{2}_{tBu}$	110	3	0[e]	0	0	0	0	0
				Reactions Involving $\mathbf{1}_{iPr}$					
14	[Ru$_3$(CO)$_{12}$] + $\mathbf{1}_{iPr}$	20	1	100[c]	x[f]	x[f]	x[f]	x[f]	0
15	[Ru$_3$(CO)$_{12}$] + 4 $\mathbf{1}_{iPr}$	20	1	100[c]	x[f]	0	0	x[f]	0
16	[Ru$_3$(CO)$_{12}$] + $\mathbf{1}_{iPr}$	90	2	0	0	0	0	0	100[c]
17	1/3 [Ru$_3$(CO)$_{12}$] + $\mathbf{2}_{iPr}$	90	2	0	0	0	0	0	100
18	[Ru$_3$(CO)$_{12}$] + 8 $\mathbf{1}_{iPr}$	100	3	0	100	0	0	0	0
19	$\mathbf{7}_{iPr}$ + 4 $\mathbf{1}_{iPr}$	100	1	0[e]	0	0	0	0	0
20	$\mathbf{2}_{iPr}$	110	3	0[e]	0	0	0	0	0

[a]All reactions were performed in toluene under argon (except entries 3 and 4) and were monitored by IR spectroscopy (ν_{CO} stretching region). [b]Relative molar amounts were estimated by ^{1}H NMR integration of the crude reaction mixture, assigning a value of 100 to the major reaction product. [c]The presence of [Ru$_3$(CO)$_{12}$] in the product mixture was detected by IR spectroscopy. [d]CO bubbled (1 atm). [e]Decomposition to an unidentified material was observed. [f]The relative amount of this product could not be estimated by ^{1}H NMR due to severe overlapping of signals of different products, but its presence in the crude reaction mixture was confirmed by IR spectroscopy.

reactions of [Ru$_3$(CO)$_{12}$] with monodentate P-donor ligands[1] and NHCs[2] under thermal conditions, but the nuclearity and ratio of the reaction products and their relationship with the type and ratio of the reactants have never been satisfactorily explained.

With the aim of gaining insight into the pathways followed by the above-described reactions, additional experiments were performed. Surprisingly and very importantly, the reaction of [Ru$_3$(CO)$_{12}$] with 1 equiv of $\mathbf{1}_{tBu}$ was not inhibited by the presence of CO (the gas was bubbled through the solution; Table 1, entry 3), but gave the mononuclear monogermylene $\mathbf{2}_{tBu}$ as the only reaction product. After 1 h, all $\mathbf{1}_{tBu}$ was consumed, while some [Ru$_3$(CO)$_{12}$] remained unreacted. Therefore, [Ru$_3$(CO)$_{12}$] may undergo cluster fission through an associative pathway that is independent of CO.

The fact that the trinuclear monogermylene complex $\mathbf{4}_{tBu}$ was a minor product of the reaction of entry 1 and that it was not observed in the product mixtures of the reactions of entries 2 and 3 of Table 1 led us to investigate its reactivity with CO and $\mathbf{1}_{tBu}$. We found that $\mathbf{4}_{tBu}$ is stable under CO (1 atm) at room temperature (a trace amount of [Ru$_3$(CO)$_{12}$] was the only reaction product after 2 h, Table 1, entry 4), but it reacted readily with 1 equiv of $\mathbf{1}_{tBu}$ (Table 1, entry 5) to give the mononuclear complexes $\mathbf{2}_{tBu}$ and $\mathbf{3}_{tBu}$ as major reaction products (in ca. 3/1 mol ratio) accompanied by a considerable amount of the trinuclear digermylene complex $\mathbf{5}_{tBu}$ and some trinuclear trigermylene $\mathbf{6}_{tBu}$. An increase of the amount of reagent $\mathbf{1}_{tBu}$ (Table 1, entry 6) resulted in an increase of $\mathbf{3}_{tBu}$ and $\mathbf{6}_{tBu}$ and the complete disappearance of $\mathbf{5}_{tBu}$, while the mononuclear monogermylene $\mathbf{2}_{tBu}$ was maintained as the major reaction product. Thus, $\mathbf{4}_{tBu}$ is a precursor to $\mathbf{2}_{tBu}$, $\mathbf{3}_{tBu}$, $\mathbf{5}_{tBu}$, and $\mathbf{6}_{tBu}$, but in the reaction of [Ru$_3$(CO)$_{12}$] with $\mathbf{1}_{tBu}$ some (or much) of $\mathbf{2}_{tBu}$ can also be formed directly without the intermediacy of $\mathbf{4}_{tBu}$.

The trinuclear digermylene complex $\mathbf{5}_{tBu}$ was quantitatively converted at room temperature into the trinuclear trigermylene derivative $\mathbf{6}_{tBu}$ by treating the former with an excess of $\mathbf{1}_{tBu}$ (Table 1, entry 7). This experiment also confirmed that $\mathbf{5}_{tBu}$ and $\mathbf{6}_{tBu}$ are not precursors to the mononuclear complexes $\mathbf{2}_{tBu}$ and $\mathbf{3}_{tBu}$ at room temperature, even in the presence of $\mathbf{1}_{tBu}$.

Interestingly, the above-described scenario changed completely when the reactions were performed at higher temperature (90−100 °C). Thus, the treatment of [Ru$_3$(CO)$_{12}$] with 1 equiv of $\mathbf{1}_{tBu}$ at 90 °C (Table 1, entry 8) led only to two trinuclear products, namely, the monogermylene derivative $\mathbf{4}_{tBu}$ (major product) and the digermylene derivative $\mathbf{5}_{tBu}$ (some [Ru$_3$(CO)$_{12}$] remained unreacted). Therefore, as the mononuclear germylene complex $\mathbf{2}_{tBu}$ should be the first product formed in this reaction (it is formed at room temperature, see above), it should react with [Ru$_3$(CO)$_{12}$] at 90 °C to give the triruthenium monogermylene derivative $\mathbf{4}_{tBu}$. This proposal was subsequently verified by treating $\mathbf{2}_{tBu}$ with 2/3 equiv of [Ru$_3$(CO)$_{12}$] at 90 °C (Table 1, entry 9), since this reaction quantitatively led to compound $\mathbf{4}_{tBu}$.

At room temperature, the reaction of [Ru$_3$(CO)$_{12}$] with a large excess (8 equiv) of $\mathbf{1}_{tBu}$ led to a ca. 2:1 mixture of the mononuclear complexes $\mathbf{2}_{tBu}$ and $\mathbf{3}_{tBu}$ as well as a small amount of $\mathbf{6}_{tBu}$, leaving intact ca. 4 equiv of $\mathbf{1}_{tBu}$ in the reaction solution.

DOI: 10.1021/acs.inorgchem.5b00084
Inorg. Chem. 2015, 54, 2983−2994

When this solution was heated at 100 °C, $\mathbf{3}_{tBu}$ was observed as the only final product (Table 1, entry 10). This fact implied that both $\mathbf{2}_{tBu}$ and $\mathbf{6}_{tBu}$ should also react with $\mathbf{1}_{tBu}$ at high temperature to give $\mathbf{3}_{tBu}$. This was subsequently confirmed by treating $\mathbf{2}_{tBu}$ and $\mathbf{6}_{tBu}$ with $\mathbf{1}_{tBu}$ at 100 °C (Table 1, entries 11 and 12).

Finally, we heated a toluene solution of the mononuclear monogermylene complex $\mathbf{2}_{tBu}$ to reflux temperature to check whether this complex could also be a precursor to the trinuclear trigermylene derivative $\mathbf{6}_{tBu}$ upon thermal decarbonylation and subsequent trimerization (Table 1, entry 13). However, the thermolysis of $\mathbf{2}_{tBu}$ slowly led to a very dark brown suspension that did not contain any previously identified complex.

Reactions Involving Ge(^{i}Pr$_2$bzam)^{t}Bu ($\mathbf{1}_{iPr}$). The IR spectra in the ν_{CO} region of the solutions obtained by treating $[Ru_3(CO)_{12}]$ with 1 and 4 equiv of $\mathbf{1}_{iPr}$ in toluene at room temperature (Table 1, entries 14 and 15) were comparable to those described above using $\mathbf{1}_{tBu}$ instead of $\mathbf{1}_{iPr}$ (Table 1, entries 1 and 2). This fact confirmed that both germylenes $\mathbf{1}_{tBu}$ and $\mathbf{1}_{iPr}$ gave analogous reaction mixtures in their reactions with $[Ru_3(CO)_{12}]$ at room temperature, but, in the case of $\mathbf{1}_{iPr}$, we were unable to unambiguously quantify the relative amounts of each complex in the reaction mixtures because the ^{1}H NMR signals of the isopropyl and tertbutyl groups of the trinuclear complexes (minor products) were overlapped with those of the mononuclear complexes (major products), hampering a reliable integration of the signals of each product in the mixture. This fact prevented us from repeating all the reactions with $\mathbf{1}_{iPr}$ that we performed with $\mathbf{1}_{tBu}$.

Interestingly, when the reaction of $[Ru_3(CO)_{12}]$ with 1 equiv of $\mathbf{1}_{iPr}$ was performed at 90 °C (Table 1, entry 16), the binuclear monogermylene $\mathbf{7}_{iPr}$ was the only reaction product after 1 h. While some $[Ru_3(CO)_{12}]$ was observed at the end of this reaction, the trinuclear monogermylene $\mathbf{4}_{iPr}$ was detected by IR as a transient intermediate. We also prepared $\mathbf{7}_{iPr}$ in quantitative yield by reacting $\mathbf{2}_{iPr}$ with 1/3 equiv of $[Ru_3(CO)_{12}]$ in toluene at 90 °C (Table 1, entry 17), and again, the trinuclear monogermylene $\mathbf{4}_{iPr}$ was detected by IR as a transient intermediate. However, as occurred with $\mathbf{1}_{tBu}$, the treatment of $[Ru_3(CO)_{12}]$ with a large excess of $\mathbf{1}_{iPr}$ (8 equiv) in toluene at 100 °C (Table 1, entry 18) led to the corresponding mononuclear digermylene ($\mathbf{3}_{iPr}$) as the only reaction product. In this case, $\mathbf{2}_{iPr}$ was the only observed reaction intermediate ($\mathbf{4}_{iPr}$ and $\mathbf{7}_{iPr}$ were not detected at any stage of the reaction). We subsequently corroborated that $\mathbf{7}_{iPr}$ is not a precursor to the mononuclear species $\mathbf{2}_{iPr}$ and $\mathbf{3}_{iPr}$, since the treatment of $\mathbf{7}_{iPr}$ with an excess of $\mathbf{1}_{iPr}$ (4 equiv) in toluene at 100 °C (Table 1, entry 19) gave a complex mixture of unidentified products.

Finally, as in the case of the mononuclear monogermylene $\mathbf{2}_{tBu}$, the thermolysis of $\mathbf{2}_{iPr}$ in toluene at reflux temperature slowly led to extensive decomposition (Table 1, entry 20), probably due to the low thermal stability of the germylene ligand.

A discussion of all these reactivity results in the context of the hitherto reported reactivity of $[Ru_3(CO)_{12}]$ with other two-electron-donor ligands, such as trialkylphosphines and NHCs, is provided in the following pages.

Structural Analysis of the Reaction Products. All isolated products were characterized by elemental analysis, mass spectrometry, IR and NMR spectroscopies, and in some cases ($\mathbf{3}_{iPr}$, $\mathbf{4}_{tBu}$, $\mathbf{6}_{iPr}$, and $\mathbf{7}_{iPr}$) by single-crystal X-ray diffraction. Complete analytical data are given in the Experimental Section of this paper (graphical NMR spectra are given as Supporting Information). As the types of compounds described in this paper are structurally unexceptional (complexes of these types having other two-electron-donor ligands have already been reported), the following paragraphs are only devoted to the particular X-ray diffraction and spectroscopic features that are directly associated with the presence of the amidinatogermylene ligands in these complexes.

The molecular structures of $\mathbf{3}_{iPr}$, $\mathbf{4}_{tBu}$, $\mathbf{6}_{iPr}$, and $\mathbf{7}_{iPr}$, determined by single-crystal X-ray diffraction, are shown in Figures 2–5. Selected bond distances are given in the figure captions. They all confirm the structures proposed for these complexes in Figure 1. In the crystal, compound $\mathbf{3}_{iPr}$ displays C_2 symmetry (Figure 2). To minimize steric interactions between the germylenes and the CO ligands, the Ru–Ge1 and Ru–Ge1* bonds are not colinear, the Ge1–Ru–Ge1* bond angle being 170.51(2)°. A similar situation was found in [Ru{Ge(HMDS)$_2$}$_2$(CO)$_3$] (HMDS = N(SiMe$_3$)$_2$), which is the only ruthenium carbonyl complex having a terminal germylene ligand whose structure has been previously determined by X-ray diffraction crystallography.[11e] In complexes $\mathbf{4}_{tBu}$ (Figure 3) and $\mathbf{6}_{iPr}$ (Figure 4), the germylene ligands are similarly located on equatorial coordination sites of their corresponding triruthenium cluster. The molecule of $\mathbf{6}_{iPr}$ displays a non-crystallographic C_3 symmetry, having the three benzamidinate groups positioned at the same side of the Ru$_3$ plane.

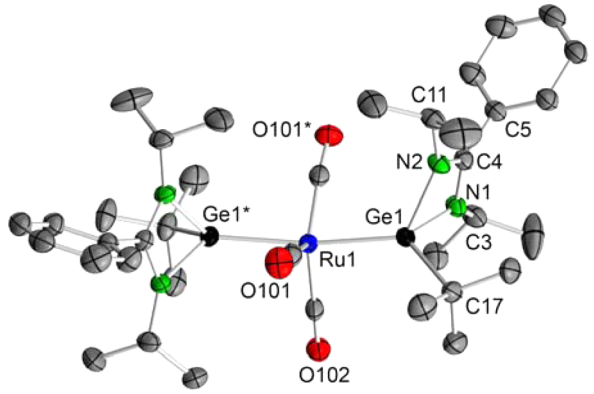

Figure 2. X-ray diffraction molecular structure of $\mathbf{3}_{iPr}$. Thermal ellipsoids set at 40% probability. H atoms were omitted for clarity. Selected bond lengths (Å) and angles (deg): Ru1–Ge1 2.3988(4), Ge1–C17 1.9998(3), Ge1–N1 1.988(3), Ge1–N2 1.999(3), N1–C3 1.463(5), N1–C4 1.335(4), N2–C4 1.317(4), N2–C11 1.466(4), C4–C5 1.484(5); Ru1–Ge1–N1 119.22(9), Ru1–Ge1–N2 119.87(9), C17–Ge1–Ru1 126.9(1), C17–Ge1–N1 104.3(2), C17–Ge1–N2 104.2(1), N1–Ge1–N2 66.1(1), Ge1–N1–C4 91.7(2), Ge1–N2–C4 91.8(2), N1–C4–N2 110.1(3), Ge1–Ru1–Ge1* 170.51(2).

The molecular structure of $\mathbf{7}_{iPr}$ (Figure 5) is entirely analogous to that of [Ru$_2${μ-κ^2-*Ge,N*-Ge(^{i}Pr$_2$bzam)(HMDS)}(CO)$_7$],[12] but the former has a *tert*-butyl group (instead of an HMDS group) attached to the Ge atom. Both isopropyl groups of $\mathbf{7}_{iPr}$ have their central CH hydrogen atoms close to the benzamidinate phenyl ring, which is perpendicular to the N1–C4–N2 and Ru1–Ru2–Ge1 planes. This situation minimizes steric interactions not only between the phenyl and isopropyl groups but also between the tertbutyl methyl groups and its closest isopropyl methyl groups. These binuclear complexes, in which the amidinatogermylenes act as 4-electron-donor κ^2-

DOI: 10.1021/acs.inorgchem.5b00084
Inorg. Chem. 2015, 54, 2983–2994

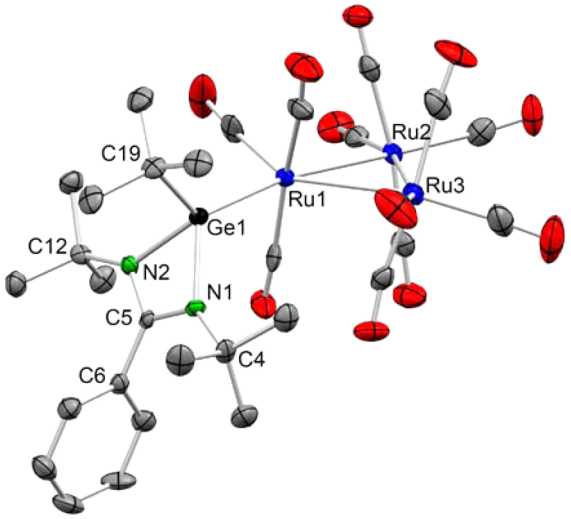

Figure 3. X-ray diffraction molecular structure of $\mathbf{4}_{tBu}$. Thermal ellipsoids set at 60% probability. H atoms were omitted for clarity. Selected bond lengths (Å) and angles (deg): Ru1−Ru2 2.8504(6), Ru1−Ru3 2.8834(6), Ru2−Ru3 2.8418(6), Ru1−Ge1 2.4363(7), Ge1−C19 2.007(5), Ge1−N1 1.984(4), Ge1−N2 1.993(4), N1−C4 1.493(6), N1−C5 1.338(6), N2−C5 1.331(6), N2−C12 1.475(7), C5−C6 1.486(7); Ru1−Ge1−N1 120.2(1), Ru1−Ge1−N2 116.3(1), C19−Ge1−Ru1 126.2(1), C19−Ge1−N1 106.8(2), C19−Ge1−N2 104.9(2), N1−Ge1−N2 66.6(2), Ge1−N1−C5 91.9(3), Ge1−N2−C5 91.8(3), N1−C5−N2 109.7(4).

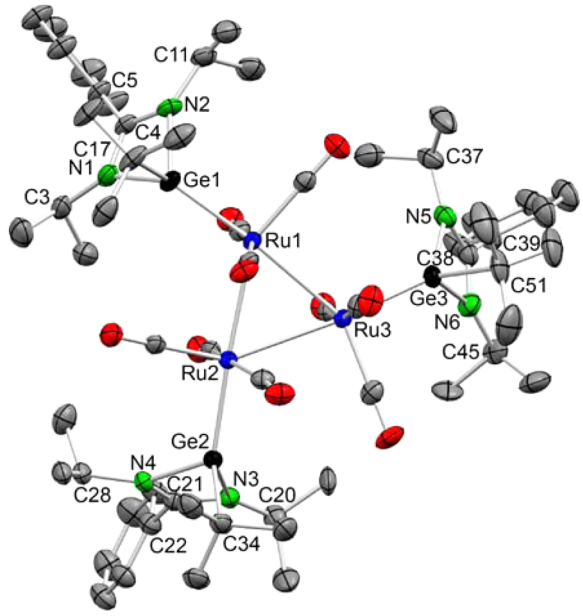

Figure 4. X-ray diffraction molecular structure of $\mathbf{6}_{iPr}$. Thermal ellipsoids set at 40% probability. H atoms were omitted for clarity, and only one of the two positions in which the two disordered isopropyl groups (C20 and C45 are their methine carbon atoms) were found is shown. Selected bond lengths (Å) and angles (deg): Ru1−Ru2 2.8756(6), Ru1−Ru3 2.8706(5), Ru2−Ru3 2.8781(6), Ru1−Ge1 2.3984(7), Ru2−Ge2 2.4052(7), Ru3−Ge3 2.3955(8), Ge1−C17 2.015(6), Ge1−N1 1.999(5), Ge1−N2 2.002(5), N1−C3 1.473(9), N1−C4 1.322(8), N2−C4 1.324(8), N2−C11 1.464(9), C4−C5 1.493(8), Ge2−C34 2.019(6), Ge2−N3 2.014(5), Ge2−N4 1.989(5), N3−C21 1.329(8), N4−C21 1.314(8), N4−C28 1.464(8), C21−C22 1.493(9), Ge3−C51 2.003(7), Ge3−N5 1.988(5), Ge3−N6 2.012(6), N5−C37 1.448(9), N5−C38 1.326(8), N6−C38 1.317(9), C38−C39 1.49(1) (the N3−C20 and N6−C45 bond distances are not given because C20 and C45 atoms are involved in positional disorder); Ru1−Ge1−N1 123.2(2), Ru1−Ge1−N2 116.7(2), C17−Ge1−Ru1 127.0(2), C17−Ge1−N1 104.5(3), C17−Ge1−N2 102.3(2), N1−Ge1−N2 65.9(2), Ge1−N1−C4 91.7(4), Ge1−N2−C4 91.5(4), N1−C4−N2 110.7(5), Ru2−Ge2−N3 123.4(2), Ru2−Ge2−N4 117.6(2), C34−Ge2−Ru2 126.9(2), C34−Ge2−N3 103.3(2), C34−Ge2−N4 102.9(2), N3−Ge2−N4 65.6(2), Ge2−N3−C21 91.2(4), Ge2−N4−C21 92.8(4), N3−C21−N4 110.3(5), Ru3−Ge3−N5 126.4(2), Ru3−Ge3−N6 116.8(2), C51−Ge3−Ru3 125.9(3), C51−Ge3−N5 102.8(3), C51−Ge3−N6 101.6(3), N5−Ge3−N6 65.9(2), Ge3−N5−C38 92.0(4), Ge3−N6−C38 91.2(4), N5−C38−N6 110.9(6).

N,Ge-ligands,[12−14] are rare exceptions to the general two-electron-donor behavior of amidinato-HT ligands.[9,15]

A notable feature of the IR spectra of the complexes involved in this work is that they present their ν_{CO} absorptions at very low frequencies. For comparison purposes, Table 2 contains IR ν_{CO} data of four groups of ruthenium carbonyl complexes that contain two-electron-donor ligands and that are structurally analogous to $\mathbf{2}_R$, $\mathbf{3}_R$, $\mathbf{4}_R$, and $\mathbf{6}_R$.[3d,4,16−20] These data demonstrate that the amidinatogermylenes used is this work ($\mathbf{1}_{tBu}$ and $\mathbf{1}_{iPr}$) are ligands of remarkable basicity, their electron-donating character being even higher than those of trialkylphosphines and comparable in some cases with those of N-heterocyclic carbenes (NHCs). Table 2 also indicates that $\mathbf{1}_{tBu}$ is a slightly stronger electron-donor than $\mathbf{1}_{iPr}$.

While the room-temperature ^{1}H and ^{13}C{^{1}H} NMR spectra of compounds $\mathbf{2}_R$−$\mathbf{6}_R$ display the resonances of a symmetric (mirror symmetry) amidinatogermylene ligand in which the two benzamidinate N−R groups of each ligand are equivalent, the corresponding spectra of compound $\mathbf{7}_{iPr}$ clearly indicate that its two isopropyl groups are nonequivalent, reflecting the asymmetry of this complex.

Density Functional Theory Calculation of Thermodynamic Parameters. Table 3 contains the density functional theory (DFT)-calculated Gibbs energies at two temperatures, 298.15 and 363.15 K, computed at the wB97XD/LanL2DZ/6-31G(d,p) level and corrected for solvation effects (CPCM model, toluene), for selected reactions relevant to the present work.

Without exceptions, all reactions involving the free germylenes $\mathbf{1}_R$ as reactants (Table 3 entries 1−7, 10, and 12) are thermodynamically favored at both 298.15 and 363.15 K. Therefore, those that are not experimentally observed at room temperature (entries 6, 7) should be kinetically disfavored at this temperature (high energy barrier).

Of particular interest are the reactions of entries 8 ($\mathbf{2}_{tBu}$ + 2/3[$Ru_3(CO)_{12}$] → $\mathbf{4}_{tBu}$ + CO) and 11 ($\mathbf{2}_{iPr}$ + 1/3[$Ru_3(CO)_{12}$] → $\mathbf{7}_{iPr}$ + CO) of Table 3 because they imply processes never studied before for other mononuclear [$RuL(CO)_4$] complexes. In these cases, the Gibbs energies are positive at both temperatures, but their absolute values are very small. As these reactions do proceed experimentally, although only at high temperature (Table 1, entries 9 and 17), their driving force should be their irreversible release of CO (the reactions were not performed in sealed vessels), which drives their corresponding reaction equilibrium toward the right. Entry 9 of Table 3 indicates that the transformation of $\mathbf{4}_{iPr}$ into $\mathbf{7}_{iPr}$ and 1/3[$Ru_3(CO)_{12}$] should not be possible at room temperature but may occur at higher temperatures, as in fact it does (Table 1, entry 14 vs entry 16).

DOI: 10.1021/acs.inorgchem.5b00084
Inorg. Chem. 2015, 54, 2983−2994

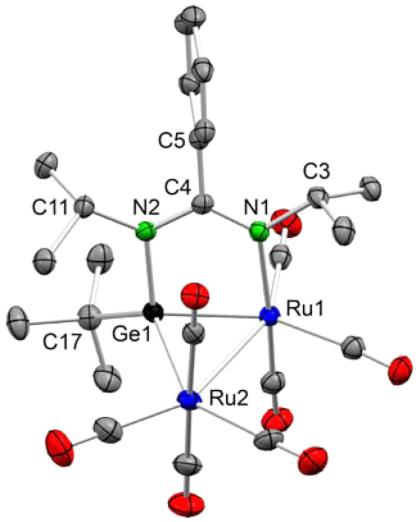

Figure 5. X-ray diffraction molecular structure of $\mathbf{7}_{iPr}$. Thermal ellipsoids set at 40% probability. H atoms were omitted for clarity. Selected bond lengths (Å) and angles (deg): Ru1−Ru2 2.9773(4), Ru1−N1 2.174(3), Ru1−Ge1 2.4073(5), Ru2−Ge1 2.5127(4), Ge1−C17 2.001(4), Ge1−N2 1.943(3), N1−C3 1.503(5), N1−C4 1.322(4), N2−C4 1.354(5), N2−C11 1.504(4), C4−C5 1.507(5); Ru1−Ge1−N2 98.44(9), Ru2−Ge1−N2 109.73(8), C17−Ge1−Ru1 126.8(1), C17−Ge1−Ru2 128.4(1), C17−Ge1−N2 111.5(1), Ru1−Ge1−Ru2 74.44(1), Ru1−Ru2−Ge1 51.16(1), Ge1−Ru1−Ru2 54.40(1), Ge1−N2−C4 115.3(2), Ru1−N1−C4 123.2(2), N1−C4−N2 122.0(3).

Table 3. Density Functional Theory-Computed Gibbs Energies for Selected Reactions[a]

No.	reaction	$\Delta G_{298.15}$	$\Delta G_{363.15}$
1	$\mathbf{1}_{tBu} + 1/3[Ru_3(CO)_{12}] \rightarrow \mathbf{2}_{tBu}$	−24.5	−23.5
2	$\mathbf{1}_{tBu} + [Ru_3(CO)_{12}] + \rightarrow \mathbf{4}_{tBu} + CO$	−22.0	−20.9
3	$\mathbf{1}_{tBu} + \mathbf{4}_{tBu} \rightarrow \mathbf{5}_{tBu} + CO$	−18.1	−16.6
4	$\mathbf{1}_{tBu} + \mathbf{5}_{tBu} \rightarrow \mathbf{6}_{tBu} + CO$	−21.2	−20.5
5	$\mathbf{1}_{tBu} + 1/3\mathbf{4}_{tBu} \rightarrow 2/3\mathbf{2}_{tBu} + 1/3\ \mathbf{3}_{tBu}$	−23.7	−22.9
6	$\mathbf{1}_{tBu} + \mathbf{2}_{tBu} \rightarrow \mathbf{3}_{tBu} + CO$	−19.5	−19.0
7	$\mathbf{1}_{tBu} + 1/3\mathbf{6}_{tBu} \rightarrow \mathbf{3}_{tBu}$	−23.5	−23.2
8	$\mathbf{2}_{tBu} + 2/3[Ru_3(CO)_{12}] \rightarrow \mathbf{4}_{tBu} + CO$	2.5	2.6
9	$\mathbf{4}_{iPr} \rightarrow \mathbf{7}_{iPr} + 1/3[Ru_3(CO)_{12}]$	0.4	−0.4
10	$\mathbf{1}_{iPr} + 2/3[Ru_3(CO)_{12}] \rightarrow \mathbf{7}_{iPr} + CO$	−22.4	−22.2
11	$\mathbf{2}_{iPr} + 1/3[Ru_3(CO)_{12}] \rightarrow \mathbf{7}_{iPr} + CO$	1.5	0.7
12	$\mathbf{1}_{iPr} + 1/3[Ru_3(CO)_{12}] \rightarrow \mathbf{2}_{iPr}$	−23.9	−22.9

[a]Data (in kcal mol^{-1}) calculated at the wB97XD/LanL2DZ/6-31G(d,p) level (toluene solvent, CPCM model).

DISCUSSION

Room Temperature Reactions. A mechanistic proposal that accounts for the experimental outcomes of reactions of $[Ru_3(CO)_{12}]$ with different amounts of the amidinatogermylenes $\mathbf{1}_{tBu}$ and $\mathbf{1}_{iPr}$ at room temperature is depicted in Scheme 2.

We propose that the first step of the reactions of $[Ru_3(CO)_{12}]$ with germylenes $\mathbf{1}_R$ is the formation of a transient adduct between these two molecules, "$[Ru_3(CO)_{12}]\cdot\mathbf{1}_R$", that may evolve by either releasing CO to give $[Ru_3(\mathbf{1}_R)(CO)_{11}]$ $(\mathbf{4}_R)$ or by breaking Ru−Ru bonds to give $[Ru(\mathbf{1}_R)(CO)_4]$ $(\mathbf{2}_R)$

Table 2. Comparative IR ν_{CO} Data

complex	L	solvent	ν_{CO} absorptions/cm^{-1}	reference
$[RuL(CO)_4]$	PPh_3	*n*-heptane	2062 (s), 1988 (m), 1953 (vs)	16
	PBu_3	*n*-heptane	2059 (s), 1983 (m), 1944 (vs)	16
	PCy_3	*n*-heptane	2056 (s), 1978 (m), 1943 (vs), 1936 (vs)	16
	IMes	nujol	2044 (s), 2007 (m), 1955 (s), 1921 (s)	4a
	$\mathbf{1}_{tBu}$	toluene	2042 (s), 1965 (m), 1933 (vs), 1924 (vs)	this work
	$\mathbf{1}_{iPr}$	toluene	2043 (s), 1966 (m), 1927 (vs)	this work
$[RuL_2(CO)_3]$	PPh_3	*n*-heptane	1910 (s)	16
	PBu_3	*n*-heptane	1890 (s)	16
	PCy_3	*n*-heptane	1882 (s), 1867 (s)	16
	IMes	KBr	1950, 1879, 1830[a]	17
	ICy	C_6D_6	2009, 1930, 1870, 1839[a]	18
	IEt_2Me_2	C_6D_6	1931 (w), 1833 (vs)	4b
	IMe_4	nujol	1840 (vs)	19
	$\mathbf{1}_{tBu}$	toluene	1937 (w), 1868 (vs), 1852 (vs)	this work
	$\mathbf{1}_{iPr}$	toluene	1939 (w), 1867 (vs), 1853 (vs)	this work
$[Ru_3L(CO)_{11}]$	PPh_3	*c*-hexane	2097 (m), 2047 (m), 2031 (sh), 2026 (sh), 2017 (s), 2001 (w), 1986 (w)	3d
	PCy_3	*c*-hexane	2082 (m), 2047 (s), 2026 (s), 2016 (vs), 1996 (s), 1985 (s), 1970 (m), 1945 (m)	21
	PMe_3	*c*-hexane	2086 (m), 2066 (sh), 2056 (m), 2040 (s), 2023 (s), 2011 (vs), 1990 (sh), 1978 (sh), 1943 (m)	21
	a-I*Ad*	nujol	2094, 2068, 2036, 2019, 2000, 1988, 1982, 1967, 1960, 1927[a]	4c
	a-I*t*Bu	KBr	2085 (m), 2034 (s), 2013 (s), 1996 (s), 1984 (s), 1977 (sh), 1962 (m), 1943 (m)	4d
	IMes	CH_2Cl_2	2090 (m), 2035 (s), 2020 (s), 2008 (s), 1971 (w)	4e
	IMe	CH_2Cl_2	2093 (m), 2038 (s), 2019 (s), 2005 (vs), 1975 (w), 1949 (w)	4e
	$\mathbf{1}_{tBu}$	toluene	2091 (m), 2040 (s), 2017 (s), 2007 (vs), 1980 (m), 1934 (w), 1921 (w)	this work
$[Ru_3L_3(CO)_9]$	PPh_3	*c*-hexane	2044 (m), 1978 (sh), 1967 (vs),	20
	PMe_3	*c*-hexane	2044 (w), 2015 (sh), 1997 (sh), 1975 (sh), 1943 (vs)	20
	$\mathbf{1}_{tBu}$	toluene	2020 (w), 1954 (vs), 1946 (vs), 1921 (vs)	this work
	$\mathbf{1}_{iPr}$	toluene	2025 (w), 1962 (vs), 1955 (vs), 1925 (vs)	this work

[a]No information on band intensity available.

DOI: 10.1021/acs.inorgchem.5b00084
Inorg. Chem. 2015, 54, 2983−2994

Scheme 2. Relationships between Products Arising from Reactions of $[Ru_3(CO)_{12}]$ with Amidinatogermylenes $\mathbf{1_R}$ (R = *i*Pr, ^{t}Bu) at Room Temperature[a]

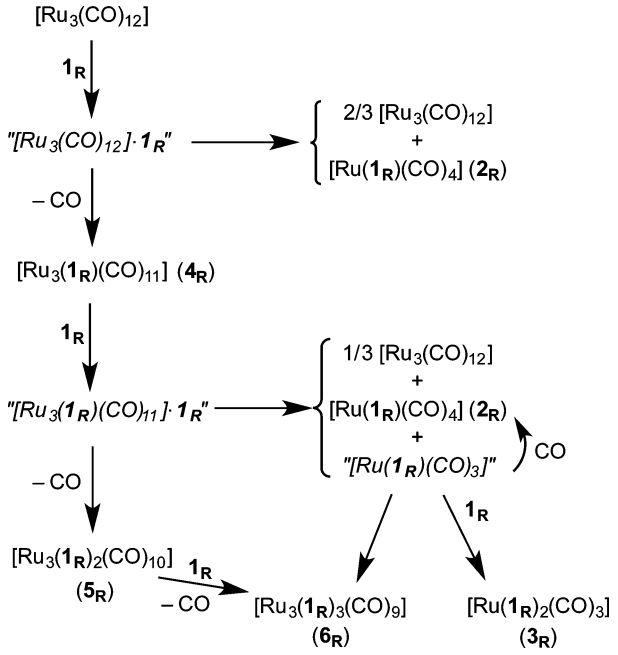

[a]Formulas in *italic* typeface represent transient unstable species.

and 2/3$[Ru_3(CO)_{12}]$ (the latter should rapidly be formed by recombination of unsaturated "$[Ru_2(CO)_8]$" and/or "$[Ru(CO)_4]$" species). Similarly, we propose that the reaction of $\mathbf{4_R}$ with $\mathbf{1_R}$ also proceeds through a transient adduct, "$[Ru_3(\mathbf{1_R})(CO)_{11}]\cdot\mathbf{1_R}$" that may also evolve by either releasing CO to give $[Ru_3(\mathbf{1_R})_2(CO)_{10}]$ ($\mathbf{5_R}$) or by breaking Ru–Ru bonds to give 1/3$[Ru_3(CO)_{12}]$, more $[Ru(\mathbf{1_R})(CO)_4]$ ($\mathbf{2_R}$), and the unsaturated species "$[Ru(\mathbf{1_R})(CO)_3]$". The latter should be very unstable and should react rapidly with either CO (some may be available because it was released to the solution during the formation of $\mathbf{4_R}$), to give more $\mathbf{2_R}$, or with $\mathbf{1_R}$ (if available) to give the mononuclear digermylene complex $[Ru(\mathbf{1_R})_2(CO)_3]$ ($\mathbf{3_R}$). In the absence of CO and $\mathbf{1_R}$, "$[Ru(\mathbf{1_R})(CO)_3]$" should undergo trimerization to give $[Ru_3(\mathbf{1_R})_3(CO)_9]$ ($\mathbf{6_R}$). The reaction of the trinuclear digermylene complex $\mathbf{5_R}$ with $\mathbf{1_R}$ (if available) may also provide more $\mathbf{6_R}$ (this may also take place through an intermediate adduct of the type "$[Ru_3(\mathbf{1_R})_2(CO)_{10}]\cdot\mathbf{1_R}$", not depicted in Scheme 2). If all reactions displayed in Scheme 2 are possible at room temperature, the ratio of the final reaction products should depend on the rate of each particular reaction step and on the ratio of the reactants.

The key features of this reaction pathway (Scheme 2) are the participation of the intermediate adducts "$[Ru_3(CO)_{12}]\cdot\mathbf{1_R}$" and "$[Ru_3(\mathbf{1_R})(CO)_{11}]\cdot\mathbf{1_R}$" and the proposal that, in addition to releasing CO to give the corresponding CO-substituted trinuclear derivatives, these adducts can spontaneously undergo cluster fission liberating mononuclear germylene species.

Regarding the nature of the intermediate trinuclear adducts, the attack of anionic nucleophiles (Nu^-, such as hydride, alkoxides, or amides) to $[Ru_3(CO)_{12}]$ and $[Os_3(CO)_{12}]$ at the C atom of a CO ligand (to form a transient anionic trinuclear derivative containing an acyl κ^1-C(O)Nu ligand) was proposed by Kaesz and co-workers as a key step in Nu^--promoted CO-substitution reactions on these clusters;[21] however, the corresponding anionic clusters $[M_3\{C(O)Nu\}(CO)_{11}]^-$ (M = Ru, Os) have never been isolated. In the case of neutral nucleophiles, the formation of a weak acid–base adduct between the nucleophile (Nu) and the C atom of a CO ligand was proposed by Morris and Basolo as a key step of Nu-promoted CO-substitution reactions on $[Fe(CO)_2(NO)_2]$;[22] however, it has not been until very recently that Huynh, Leong, and co-workers have succeeded in isolating and fully characterizing by X-ray diffraction the first adducts between neutral two-electron-donor nucleophiles and carbonyl ligands.[23] Studying the reactivity of $[Os_3(CO)_{12}]$ with bulky NHCs at room temperature, they were able to isolate various "acyl" trinuclear adducts of the type $[Os_3\{C(O)NHC\}(CO)_{11}]$ and to prove that these adducts slowly liberate CO to give $[Os_3(NHC)(CO)_{11}]$ derivatives. No mononuclear derivatives were formed in this case, probably because Os–Os bonds are quite strong, and hence cluster fission does not occur at mild temperatures.[24]

50-Electron reaction intermediates of general formula $[Ru_3L(CO)_{12}]$, which would result from the opening of an edge of the $[Ru_3(CO)_{12}]$ metal triangle upon an associative attack of the incoming nucleophile (L) to a metal atom, have also been proposed to explain CO-substitution reactions in this cluster,[25] but intermediates of this type have never been experimentally verified.

Although we were unable to isolate or even detect the adducts formulated as "$[Ru_3(CO)_{12}]\cdot\mathbf{1_R}$" and "$[Ru_3(\mathbf{1_R})(CO)_{11}]\cdot\mathbf{1_R}$" in Scheme 2, the participation of these species in the reactions studied in this contribution is clear because the processes that involve cluster fission are substrate-promoted. Given the similar characteristics (high basicity, large volume) of NHCs and the germylenes used in this work, we believe that the "acyl" structures depicted in Figure 6 may well represent

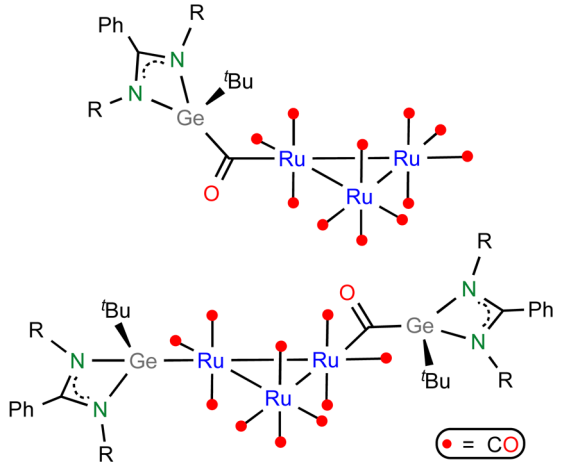

Figure 6. Proposed structures for the adducts labeled "$[Ru_3(CO)_{12}]\cdot\mathbf{1_R}$" (upper) and "$[Ru_3(\mathbf{1_R})(CO)_{11}]\cdot\mathbf{1_R}$" (lower) in Scheme 2 (R = ^{t}Bu, ^{i}Pr).

the structures of the adducts "$[Ru_3(CO)_{12}]\cdot\mathbf{1_R}$" and "$[Ru_3(\mathbf{1_R})(CO)_{11}]\cdot\mathbf{1_R}$". These neutral zwitterionic species should have a negative charge at the metallic core and a positive charge at the acyl germylene fragment.[23]

Our proposal (Scheme 2) helps justify (a) why the mononuclear monogermylene complexes $[Ru(\mathbf{1_R})(CO)_4]$ ($\mathbf{2_R}$) were always the major products of the reactions of $[Ru_3(CO)_{12}]$ with $\mathbf{1_R}$ at room temperature, regardless of the ratio of the reactants (Table 1, entries 1, 2, 14, and 15); (b) the

DOI: 10.1021/acs.inorgchem.5b00084
Inorg. Chem. 2015, 54, 2983–2994

additional formation of smaller amounts of $\mathbf{3_R}$–$\mathbf{6_R}$ in the reactions of $[Ru_3(CO)_{12}]$ with only 1 equiv of $\mathbf{1_R}$ (Table 1, entries 1 and 14); (c) the fact that $\mathbf{2_{tBu}}$ was the only product of the reaction of $[Ru_3(CO)_{12}]$ with $\mathbf{1_{tBu}}$ under CO (Table 1, entry 3); (d) the fact that $\mathbf{4_{tBu}}$ was stable under CO (Table 1, entry 4) but reacted with $\mathbf{1_{tBu}}$ to give $\mathbf{2_{tBu}}$ and $\mathbf{3_{tBu}}$ (Table 1, entries 5 and 6); (e) the fact that $\mathbf{4_{tBu}}$ reacted with $\mathbf{1_{tBu}}$ (Table 1, entries 5 and 6) to give higher yields of $\mathbf{3_{tBu}}$ (compared with those of $\mathbf{2_{tBu}}$) than the reactions of $[Ru_3(CO)_{12}]$ with $\mathbf{1_{tBu}}$ (Table 1, entries 1 and 2).

Studying reactions of $[Ru_3(CO)_{12}]$ with PBu_3 (Bu = *n*-butyl), Poë and Twigg obtained $[Ru(PBu_3)(CO)_4]$, $[Ru(PBu_3)_2(CO)_3]$, and $[Ru_3(PBu_3)_3(CO)_9]$ as reaction products in ratios that depended on the initial ratio of the reagents; high $[Ru_3(CO)_{12}]$-to-PBu_3 ratios led to more trinuclear product, while low ratios led to more mononuclear products.[3f] When mainly mononuclear products were formed, a ca. 1:2 ratio of $[Ru(PBu_3)_2(CO)_3]$ to $[Ru(PBu_3)(CO)_4]$ was obtained, and this was justified by proposing that the cluster fission should occur in $[Ru_3(PBu_3)(CO)_{11}]$ (this trinuclear complex was proposed as the first intermediate product, but it was not observed) to give "*[Ru(PBu$_3$)(CO)$_3$]*" and two "*[Ru(CO)$_4$]*" fragments that subsequently would react with PBu_3 to finally give $[Ru(PBu_3)_2(CO)_3]$ and $[Ru(PBu_3)(CO)_4]$ in a 1:2 ratio, whereas at high initial $[Ru_3(CO)_{12}]$ to PBu_3 ratios the unsaturated "*[Ru(PBu$_3$)(CO)$_3$]*" and "*[Ru(CO)$_4$]*" species would have a strong tendency to trimerize rather than to add an additional ligand, preferably giving $[Ru_3(PBu_3)_3(CO)_9]$ and $[Ru_3(CO)_{12}]$ (Scheme 3).[3f] However, Poë and Twigg's

Scheme 3. Poë and Twigg's Proposal to Explain the Reactivity of $[Ru_3(CO)_{12}]$ with PBu_3

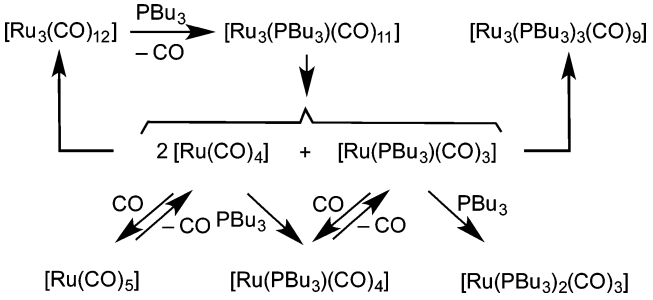

proposal (a) does not justify the cases in which the $[RuL_2(CO)_3]$ to $[RuL(CO)_4]$ ratios differ from 1:2 (as are the reactions described in this paper); (b) is also unable to rationalize why $[Ru_3L(CO)_{11}]$ is stable under CO (Table 1, entry 4), since it predicts the formation of $[RuL(CO)_4]$ and $[Ru_3(CO)_{12}]$; and (c) does not explain why $[Ru_3(CO)_{12}]$ does react with L in the presence of CO to give $[RuL(CO)_4]$ (Table 1, entry 3), since $[Ru_3L(CO)_{11}]$ should not be formed from $[Ru_3(CO)_{12}]$ and L under CO.

Subsequently, studying the reactions of the individual clusters $[Ru_3(PBu_3)_x(CO)_{12-x}]$ (x = 1–3) with PBu_3, Brodie and Poë demonstrated that all these clusters may undergo both formal CO-substitution (to give trinuclear derivatives) and associative cluster-scission (to give mononuclear derivatives) depending on the reaction conditions.[3f]

Our proposal (Scheme 2) is not only compatible with the experimental results on the reactivity of $[Ru_3(CO)_{12}]$ with PBu_3 but is also valid to explain the outcomes of reactions of $[Ru_3(CO)_{12}]$ with other phosphines of high basicity (such as PEt_2Ph,[3b] PEt_3,[3b] $PMePh_2$,[3d] and PCy_3[3d]), in which the formation of mononuclear products seems to be favored at room temperature (in each case, the product ratio should depend upon the ratio of the reactants and upon the rates of each particular reaction step, which, in turn, should depend upon the basicity and volume of the ligands). Less basic P-donor ligands, such as PPh_3, $P(OPh)_3$, or $P(OCH_2)_3CEt$ do not give mononuclear products at mild temperatures.[3e] A kinetic analysis of the reaction of $[Ru_3(CO)_{12}]$ with PPh_3 indicated that it follows a dissociative pathway.[26] Probably, PPh_3 may not be able to attack a coordinated CO and thus form the key adduct responsible for the fission of the trinuclear cluster under thermal conditions. However, upon UV irradiation, which favors metal–metal bond cleavage, the products of these reactions are $[Ru(PR_3)(CO)_4]$ and $[Ru(PR_3)_2(CO)_3]$.[27]

Concerning room-temperature reactions of $[Ru_3(CO)_{12}]$ with NHCs, some compounds of the types $[Ru(NHC)_2(CO)_3]$,[4b] $[Ru(NHC)(CO)_4]$,[4a] and $[Ru_3(NHC)(CO)_{11}]$[4c–f] have been isolated using 1:6, 1:3, and 1:1, reactant ratios, respectively, but inseparable mixtures of products have been reported to be formed when other reactant ratios were used. These results can be explained if all the initial reaction adduct "*[Ru$_3$(CO)$_{12}$]·NHC*" evolves toward $[Ru(NHC)(CO)_4]$ and 2/3$[Ru_3(CO)_{12}]$ (Scheme 2) and if $[Ru(NHC)(CO)_4]$ is able to react with more NHC to give $[Ru(NHC)_2(CO)_3]$. If there is no more NHC available, $[Ru(NHC)(CO)_4]$ may react with $[Ru_3(CO)_{12}]$ to give $[Ru_3(NHC)(CO)_{11}]$. In our case, we observed similar reactions, albeit at a higher temperature, between $\mathbf{2_{tBu}}$ and $\mathbf{1_{tBu}}$, to give $\mathbf{3_{tBu}}$ (Table 1, entry 11; Scheme 4), and between $\mathbf{2_{tBu}}$ and $[Ru_3(CO)_{12}]$, to give $\mathbf{4_{tBu}}$ (Table 1,

Scheme 4. Reactions Involving Germylene-Containing Ruthenium Carbonyl Complexes That Do Not Occur at Room Temperature but Take Place at 90–100 °C

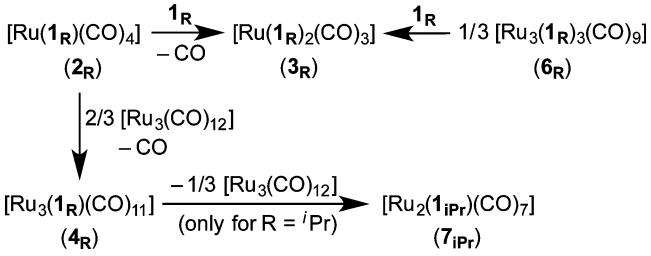

entry 9; Scheme 4). The higher basicity of NHCs may allow these reactions to occur at room temperature. This proposal also explains why no trinuclear $[Ru_3(NHC)(CO)_{11}]$ complexes were formed when 1:3 and 1:6 ratios of $[Ru_3(CO)_{12}]$ to NHC were used. Above room temperature, the reactions of $[Ru_3(CO)_{12}]$ with NHCs are known to give cyclometalated derivatives that arise from intramolecular C–H and C–N bond-activation processes.[4c,d,f,28]

High-Temperature Reactions. At higher temperatures, additional processes having higher activation barriers are also possible. In fact, the outcomes of reactions of $[Ru_3(CO)_{12}]$ with different amounts of $\mathbf{1_R}$ at 90–100 °C (Table 1, entries 8–12 and 16–18) were very different from those obtained at room temperature. Scheme 4 clearly indicates that the mononuclear digermylene $\mathbf{3_R}$ is the thermodynamically controlled product when an excess of $\mathbf{1_R}$ is available, no matter whether the ruthenium starting material is $[Ru_3(CO)_{12}]$ or $\mathbf{2_R}$–$\mathbf{6_R}$, because both $\mathbf{2_R}$ and $\mathbf{6_R}$ were transformed at 90–100 °C

DOI: 10.1021/acs.inorgchem.5b00084
Inorg. Chem. 2015, 54, 2983–2994

into $\mathbf{3_R}$ in the presence of $\mathbf{1_R}$. In the absence of free germylene, $\mathbf{2_R}$ reacted with $[Ru_3(CO)_{12}]$ at 100 °C to give $\mathbf{4_R}$ (Table 1, entry 9), while $\mathbf{4_{tBu}}$ was stable at the working temperature, $\mathbf{4_{iPr}}$ spontaneously decomposed to give the binuclear derivative $\mathbf{7_{iPr}}$ and $1/3[Ru_3(CO)_{12}]$ (Table 1, entry 17). Therefore, the thermodynamically controlled products at high $[Ru_3(CO)_{12}]$-to-$\mathbf{1_{tBu}}$ or -$\mathbf{1_{iPr}}$ ratios (≥1) are $\mathbf{4_{tBu}}$ or $\mathbf{7_{iPr}}$, respectively.

The discovery that trinuclear complexes of the type $[Ru_3L(CO)_{11}]$ may in many cases arise from the condensation of mononuclear $[RuL(CO)_4]$ complexes with $2/3[Ru_3(CO)_{12}]$ and not from a direct CO-substitution reaction on $[Ru_3(CO)_{12}]$ is a very important result because, despite the great amount of work already done on reactions of $[Ru_3(CO)_{12}]$ with two-electron-donor reagents, such a process has never been observed or even proposed before, although it rationalizes hitherto unexplained experimental results. As commented above, the selective formation of trinuclear $[Ru_3(NHC)(CO)_{11}]$ complexes upon treatment of $[Ru_3(CO)_{12}]$ with various NHCs in 1:1 mol ratio[4e] can be explained if the initially formed mononuclear $[Ru(NHC)(CO)_4]$ species are able to react with $2/3[Ru_3(CO)_{12}]$ to give $[Ru_3(NHC)(CO)_{11}]$. This type of reaction also explains why the room-temperature treatment of $[Ru_3(CO)_{12}]$ with PBu_3 at a high reactant ratio (≥1) leads predominantly to mononuclear products but to trinuclear products at higher temperatures.[3f]

In previous works, using the HMDS-substituted germylenes $Ge(R_2bzam)(HMDS)$ as starting reagents, we have demonstrated that steric factors are responsible for the instability of binuclear germylene-bridged derivatives similar to $\mathbf{7_{iPr}}$ when both R groups of the R_2bzam fragment are *tert*-butyl groups (the amidinate N−R groups are very close to the amidinate phenyl ring).[13,14] The same steric factors are valid to explain why the *tert*-butyl analogue of $\mathbf{7_{iPr}}$ ($\mathbf{7_{tBu}}$) cannot be not prepared.

CONCLUSIONS

The study of the reactivity of $[Ru_3(CO)_{12}]$ with the amidinatogermylenes $\mathbf{1_R}$ (R = ^{t}Bu and ^{i}Pr), in addition to extending the coordination chemistry of amidinatogermylenes to mononuclear ($\mathbf{2_R}$ and $\mathbf{3_R}$) and trinuclear ($\mathbf{4_R}$, $\mathbf{5_R}$, and $\mathbf{6_R}$) ruthenium carbonyl derivatives, has allowed the observation of a wide reaction panorama that includes the relationships between all the possible reaction products at room (Scheme 2) and at higher (Scheme 4) temperatures.

At room temperature, the mononuclear derivatives $\mathbf{2_R}$ and $\mathbf{3_R}$ are formed by associative cluster-fission from $[Ru_3(CO)_{12}]$ ($\mathbf{2_R}$) and $\mathbf{4_R}$ ($\mathbf{2_R}$ and $\mathbf{3_R}$), while $\mathbf{4_R}$ and $\mathbf{5_R}$ are formed by direct (presumably associative) CO-substitution reactions from $[Ru_3(CO)_{12}]$ and $\mathbf{4_R}$, respectively. The trinuclear trigermylene derivative $\mathbf{6_R}$ can be formed from $\mathbf{5_R}$ (by direct CO-substitution) or from $\mathbf{4_R}$ (by associative cluster scission and trimerization of the resulting unsaturated mononuclear "*[Ru(1R)CO)3]*" species). Of particular interest is the reaction of $[Ru_3(CO)_{12}]$ with $\mathbf{1_{tBu}}$ under CO at room temperature, which, giving $\mathbf{2_{tBu}}$, has demonstrated that this mononuclear species can be formed directly from $[Ru_3(CO)_{12}]$ by an associative cluster-fission process.

At higher temperatures (90−100 °C), both $\mathbf{2_R}$ and $\mathbf{6_R}$ lead to $\mathbf{3_R}$ in the presence of excess of $\mathbf{1_R}$. These reactions are valid in explaining why the mononuclear digermylenes $\mathbf{3_R}$ are the final products of high-temperature reactions using low $[Ru_3(CO)_{12}]$-to-$\mathbf{1_R}$ ratios (≤1/6). However, the final products of reactions performed at 90 °C using high $[Ru_3(CO)_{12}]$-to-$\mathbf{1_R}$ ratios (≥1) are the trinuclear monogermylene derivative $\mathbf{4_{tBu}}$ or the binuclear monogermylene derivative $\mathbf{7_{iPr}}$, depending on the nature of $\mathbf{1_R}$ (R = ^{t}Bu or ^{i}Pr). Of particular interest are the reactions of $\mathbf{2_R}$ with $[Ru_3(CO)_{12}]$ at 90 °C, which give $\mathbf{4_R}$ (while $\mathbf{4_{tBu}}$ is stable, $\mathbf{4_{iPr}}$ subsequently leads to $\mathbf{7_{iPr}}$) because the reaction of a mononuclear complex of the type $[RuL(CO)_4]$ with $[Ru_3(CO)_{12}]$ has never been observed before for other two-electron-donor reagents, although it explains why trinuclear derivatives of the type $[Ru_3L(CO)_{11}]$ (L = triarylphosphine, NHC) are the thermodynamically controlled products of reactions involving $[Ru_3(CO)_{12}]$ to L in ratios ≥1.

Finally, Schemes 2 and 4, in addition to summarizing and explaining the results reported in this paper, can also be used as a general tool to rationalize previously reported reactions of $[Ru_3(CO)_{12}]$ with different amounts of other two-electron-donor reagents of high basicity (L), such as trialkylphosphines and NHCs.

EXPERIMENTAL SECTION

General Procedures. Solvents were dried over appropriate desiccating reagents and were distilled and kept under argon before use. All reactions were performed under argon, using drybox and/or Schlenk vacuum line techniques and were routinely monitored by solution IR spectroscopy. The germylenes $Ge(^iPr_2bzam)^tBu$ ($\mathbf{1_{iPr}}$)[11a] and $Ge(^tBu_2bzam)Cl$[29] were prepared following published procedures. All remaining reagents were purchased from commercial sources. A selection of the reactions discussed in this work is collected in Table 1. Selected synthetic procedures are given below. All reaction products were vacuum-dried for several hours prior to being weighted and analyzed. NMR spectra were run on a Bruker DPX-300 instrument; a residual protic solvent resonance was used as reference for ^{1}H [$\delta(C_6HD_5)$ = 7.16 ppm; $\delta(C_6D_5CHD_2)$ = 2.08 ppm], whereas a solvent resonance was used as reference for ^{13}C [$\delta(C_6D_6)$ = 128.1 ppm; $\delta(C_6D_5CD_3)$ = 20.4 ppm]. Microanalyses were obtained from a PerkinElmer 2400 microanalyzer. Mass spectra (MS) were run on a VG Autospec double-focusing mass spectrometer operating in the fast-atom bombardment (FAB+) mode; ions were produced with a standard Cs^+ gun at ∼30 kV; 3-nitrobenzyl alcohol was used as matrix; data given correspond to the most abundant isotopomer of the molecular ion or of the greatest mass fragment.

$Ge(^tBu_2bzam)^tBu$ ($\mathbf{1_{tBu}}$). A dibutyl ether solution of Li^{t}Bu (6.0 mL, 1.7 M, 10.2 mmol) was added to a cold (−78 °C) solution of $Ge(^tBu_2bzam)Cl$ (3.43 g, 10.1 mmol) in diethyl ether (30 mL). The resulting suspension was allowed to warm to room temperature, and then it was stirred for 6 h. The solvents were removed under reduced pressure, and the residue was extracted into hexane (3 × 30 mL). The filtrate was evaporated to dryness under vacuum to give $\mathbf{1_{tBu}}$ as a yellowish powder (3.07 g, 84%). Anal. Calcd for $C_{19}H_{32}GeN_2$ (M_W = 361.08): C, 63.20; H, 8.93; N, 7.76. Found: C, 63.22; H, 8.95; N, 7.1%. ^{1}H NMR (C_6D_6, 300.1 MHz, 293 K): δ 7.14−6.95 (m, 5 H, 5 *CH* of Ph), 1.40 (s, 9 H, 3 *Me* of ^{t}Bu), 1.03 (s, 18 H, 6 *Me* of 2 ^{t}Bu). ^{13}C{^{1}H} NMR (C_6D_6, 75.5 MHz, 293 K): δ 165.4 (s, *NCN*), 136.9 (C_{ipso} of Ph), 130.1 (s, *CH* of Ph), 129.3 (*CH* of Ph), 129.1 (*CH* of Ph), 127.7 (*CH* of Ph), 127.4 (*CH* of Ph), 52.7 (2 *C* of 2 ^{t}Bu), 32.5 (6 *Me* of 2 ^{t}Bu), 31.3 (*C* of ^{t}Bu), 28.7 (3 *Me* of ^{t}Bu).

$[Ru(1_{tBu})(CO)_4]$ ($\mathbf{2_{tBu}}$) and $[Ru(1_{tBu})_2(CO)_3]$ ($\mathbf{3_{tBu}}$). A toluene solution of $\mathbf{1_{tBu}}$ (1.10 mL, 0.30 M, 0.330 mmol) was added to a toluene (8 mL) suspension of $[Ru_3(CO)_{12}]$ (50 mg, 0.080 mmol), and the mixture was stirred at room temperature for 1 h. The initial orange color changed to red. The crude reaction solution was concentrated to ca. 2 mL and was placed at −20 °C. Some crystals appeared after 1 d, which were filtered, washed with hexane (2 × 5 mL), and dried in vacuum to give $\mathbf{3_{tBu}}$ as a white solid (58 mg, 27%). The filtered solution was evaporated to dryness under reduced pressure to give a solid residue that was washed with hexane (2 × 5 mL) to give $\mathbf{2_{tBu}}$ as a red solid (84 mg, 61%). A greater yield of $\mathbf{3_{tBu}}$ was obtained by heating a mixture of $[Ru_3(CO)_{12}]$ (25 mg, 0.040 mmol) and $\mathbf{1_{tBu}}$ (1.10 mL of

DOI: 10.1021/acs.inorgchem.5b00084
Inorg. Chem. 2015, 54, 2983−2994

a 0.30 M solution in toluene, 0.330 mmol) in toluene (8 mL) at 100 °C for 3 h. The initial orange color changed to light red. The solvents were removed under reduced pressure, and the residue was washed with hexane (2 × 5 mL) and dried in vacuum (95 mg, 88%). *Data for* $\mathbf{2}_{tBu}$: Anal. Calcd for $C_{23}H_{32}GeN_2O_4Ru$ (M_W = 574.20): C, 48.11; H, 5.62; N, 4.88. Found: C, 48.15; H, 5.65; N, 4.84%. (+)-FAB MS: *m/z* 574 $[M]^+$. IR (toluene, cm^{-1}): ν_{CO} 2042 (s), 1965 (m), 1933 (vs), 1924 (br, vs). ^1H NMR (C_6D_6, 300.1 MHz, 293 K): δ 7.38 (m, 1 C*H* of Ph), 7.04−6.87 (m, 4 H, 4 C*H* of Ph), 1.33 (s, 9 H, 3 *Me* of ^{t}Bu), 1.01 (s, 18 H, 6 *Me* of 2 ^{t}Bu). $^{13}C\{^1H\}$ NMR (C_6D_6, 75.5 MHz, 293 K): δ 207.8 (*C*Os), 169.8 (*N*CN), 133.3 (C_{ipso} of Ph), 130.1−127.7 (5 *C*H of Ph), 54.6 (2 *C* of 2 ^{t}Bu), 37.0 (*C* of ^{t}Bu), 32.0 (6 *Me* of 2 ^{t}Bu), 27.8 (3 *Me* of ^{t}Bu). *Data for* $\mathbf{3}_{tBu}$: Anal. Calcd for $C_{41}H_{64}Ge_2N_4O_3Ru$ (M_W = 907.26): C, 54.28; H, 7.11; N, 6.18. Found: C, 54.32; H, 7.17; N, 6.09%. (+)-FAB MS: *m/z* 908 $[M]^+$. IR (toluene, cm^{-1}): ν_{CO} 1937 (w), 1868 (vs), 1852 (vs). ^1H NMR (C_6D_6, 300.1 MHz, 293 K): δ 7.73 (m, H, C*H* of Ph), 7.09−6.89 (m, 4 H, 4 C*H* of Ph), 1.60 (s, 9 H, 3 *Me* of ^{t}Bu), 1.27 (s, 18 H, 6 *Me* of 2 ^{t}Bu). $^{13}C\{^1H\}$ NMR (C_6D_6, 75.5 MHz, 293 K): δ 213.6 (*C*Os), 168.1 (*N*CN), 134.8 (C_{ipso} of Ph), 130.3−127.6 (5 *C*H of Ph), 54.2 (2 *C* of 2 ^{t}Bu), 36.9 (*C* of ^{t}Bu), 32.3 (6 *Me* of 2 ^{t}Bu), 28.2 (3 *Me* of ^{t}Bu) ppm.

$[Ru(\mathbf{1}_{iPr})(CO)_4]$ ($\mathbf{2}_{iPr}$) and $[Ru(\mathbf{1}_{iPr})_2(CO)_3]$ ($\mathbf{3}_{iPr}$). A toluene solution of $\mathbf{1}_{iPr}$ (1.30 mL, 0.25 M, 0.325 mmol) was added to a toluene (8 mL) suspension of $[Ru_3(CO)_{12}]$ (50 mg, 0.080 mmol), and the mixture was stirred at room temperature for 1 h. The initial orange color changed to dark orange. The crude reaction solution was concentrated to ca. 2 mL and placed at −20 °C for 3 d. A crystalline solid precipitated, which was filtered, washed with hexane (2 × 5 mL), and dried in vacuum to give $\mathbf{3}_{iPr}$ as an off-white solid (65 mg, 32%). The filtered solution was evaporated to dryness to give a solid residue that was washed with hexane (2 × 5 mL) and dried in vacuum to give $\mathbf{2}_{iPr}$ as a dark orange solid (81 mg, 62%). A greater yield of $\mathbf{3}_{iPr}$ was obtained by heating a mixture of $[Ru_3(CO)_{12}]$ (25 mg, 0.040 mmol) and $\mathbf{1}_{iPr}$ (1.30 mL of a 0.25 M solution in toluene, 0.330 mmol) in toluene (8 mL) at 100 °C for 3 h. The initial orange color remained unchanged. The solvents were removed under reduced pressure, and the residue was washed with hexane (2 × 5 mL) and dried in vacuum (97 mg, 95%). *Data for* $\mathbf{2}_{iPr}$: Anal. Calcd for $C_{21}H_{28}GeN_2O_4Ru$ (M_W = 546.14): C, 46.18; H, 5.17; N, 5.13. Found: C, 46.23; H, 5.21; N, 5.09%. (+)-FAB MS: *m/z* 546 $[M]^+$. IR (toluene, cm^{-1}): ν_{CO} 2043 (s), 1966 (m), 1927 (vs). ^1H NMR (C_7D_8, 300.1 MHz, 293 K): δ 7.08−6.97 (m, 5 H, 5 C*H* of Ph), 3.36 (m, 2 H, 2 C*H* of 2 *i*Pr), 1.29 (s, 9 H, 3 *Me* of *t*Bu), 1.14 (d, *J* = 6.5 Hz, 6 H, 2 *Me* of *i*Pr), 0.85 (d, *J* = 6.5 Hz, 6 H, 2 *Me* of *i*Pr). $^{13}C\{^1H\}$ NMR (C_7D_8, 75.5 MHz, 293 K): δ 207.4 (*C*Os), 169.8 (*N*CN), 129.3−127.3 (C_{ipso} + 5 *C*H of Ph), 47.9 (2 *C*H of 2 ^{i}Pr), 36.8 (s, *C* of ^{t}Bu), 26.7 (3 *Me* of ^{t}Bu), 26.7 (2 *Me* of ^{i}Pr), 26.5 (2 *Me* of ^{i}Pr). *Data for* $\mathbf{3}_{iPr}$: Anal. Calcd (%) for $C_{37}H_{56}Ge_2N_4O_3Ru$ (M_W = 851.16): C, 52.21; H, 6.63; N, 6.58. Found: C, 52.26; H, 6.68; N, 6.56. (+)-FAB MS: *m/z* 852 $[M]^+$. IR (toluene, cm^{-1}): ν_{CO} 1939 (w), 1867 (vs), 1853 (vs). ^1H NMR (C_6D_6, 300.1 MHz, 293 K): δ 7.13−7.07 (m, 5 H, 5 C*H* of Ph), 3.54 (m, 2 H, 2 C*H* of 2 ^{i}Pr), 1.53 (s, 9 H, 3 *Me* of ^{t}Bu), 1.43 (d, *J* = 6.5 Hz, 6 H, 2 *Me* of ^{i}Pr), 1.04 (d, *J* = 6.5 Hz, 6 H, 2 *Me* of ^{i}Pr). $^{13}C\{^1H\}$ NMR (C_6D_6, 75.5 MHz, 293 K): δ 212.9 (*C*Os), 168.1 (*N*CN), 130.4−127.7 (C_{ipso} + 5 *C*H of Ph), 47.8 (2 *C*H of 2 ^{i}Pr), 36.6 (*C* of ^{t}Bu), 26.9 (3 *Me* of ^{t}Bu), 25.0 (2 *Me* of ^{i}Pr), 24.7 (2 *Me* of ^{i}Pr).

$[Ru_3(\mathbf{1}_{tBu})(CO)_{11}]$ ($\mathbf{4}_{tBu}$) and $[Ru_3(\mathbf{1}_{tBu})_2(CO)_{10}]$ ($\mathbf{5}_{tBu}$). A toluene solution of $\mathbf{1}_{tBu}$ (0.3 mL of a 0.30 M, 0.090 mmol) was added to a toluene (8 mL) suspension of $[Ru_3(CO)_{12}]$ (50 mg, 0.080 mmol), and the mixture was heated at 90 °C for 2 h. The initial orange color changed to dark red. Purification by flash chromatography (2 × 5 cm silica gel column packed in hexane) eluting with hexane (20 mL) and hexane/CH_2Cl_2 (3:1) (20 mL) afforded $\mathbf{4}_{tBu}$, which was isolated as a light red solid (55 mg, 71%). Subsequent elution of the column with hexane/CH_2Cl_2 (2:1) (20 mL) and hexane/CH_2Cl_2 (1:1) (20 mL) separated $\mathbf{5}_{tBu}$, which was isolated as a dark red solid (15 mg, 14%). *Data for* $\mathbf{4}_{tBu}$: Anal. Calcd for $C_{30}H_{32}GeN_2O_{11}Ru_3$ (M_W = 972.40): C, 37.05; H, 3.32; N, 2.88. Found: C, 37.21; H, 3.41; N, 2.84%. (+)-FAB MS: *m/z* 974 $[M]^+$. IR (toluene, cm^{-1}): ν_{CO} 2091 (m), 2040 (s), 2017 (s), 2007 (vs), 1980 (m), 1934 (w), 1921 (w). ^1H NMR (C_6D_6, 300.1 MHz, 293 K): δ 7.25 (m, 1 H, 1 C*H* of Ph), 6.98−6.88 (m, 4 *CH* of Ph), 1.31 (s, 9 H, 3 *Me* of ^{t}Bu), 0.96 (s, 18 H, 6 *Me* of 2 ^{t}Bu). $^{13}C\{^1H\}$ NMR (C_6D_6, 75.5 MHz, 293 K): δ 205.0 (*C*Os), 170.9 (*N*CN), 133.0 (C_{ipso} of Ph), 130.2−127.6 (5 CH of Ph), 54.3 (2 *C* of 2 ^{t}Bu), 38.0 (*C* of ^{t}Bu), 32.1 (6 *Me* of 2 ^{t}Bu), 27.8 (3 *Me* of ^{t}Bu) ppm. *Data for* $\mathbf{5}_{tBu}$: Anal. Calcd for $C_{48}H_{64}Ge_2N_4O_{10}Ru_3$ (M_W = 1305.47): C, 44.16; H, 4.94; N, 4.29. Found: C, 44.20; H, 4.98; N, 4.14%. (+)-FAB MS: *m/z* 1305 $[M]^+$. IR (toluene, cm^{-1}): ν_{CO} 2061 (m), 2002 (s), 1981 (vs, br), 1938 (m, br). ^1H NMR (C_6D_6, 300.1 MHz, 293 K): δ 7.38 (m, 1 H, 1 C*H* of Ph), 7.00−6.86 (m, 4 H, 4 C*H* of Ph), 1.47 (s, 9 H, 3 *Me* of ^{t}Bu), 1.10 (s, 18 H, 6 *Me* of 4 ^{t}Bu). $^{13}C\{^1H\}$ NMR (C_6D_6, 75.5 MHz, 293 K): δ 210.6 (*C*Os), 170.0 (*N*CN), 133.8 (C_{ipso} of Ph), 130.4−127.4 (5 CH of Ph), 54.1 (2 *C* of 2 ^{t}Bu), 37.9 (*C* of ^{t}Bu), 32.3 (6 *Me* of 2 ^{t}Bu), 28.1 (3 *Me* of ^{t}Bu).

$[Ru_3(\mathbf{1}_{tBu})_3(CO)_9]$ ($\mathbf{6}_{tBu}$). A toluene solution of $\mathbf{1}_{tBu}$ (0.55 mL of a 0.30 M, 0.165 mmol) was added to a solution of $[Ru_3(\mathbf{1}_{tBu})_2(CO)_{10}]$ ($\mathbf{5}_{tBu}$) (50 mg, 0.038 mmol) in toluene (8 mL), and the mixture was stirred at room temperature for 1 h. The initial red color remained unchanged. Purification by flash chromatography (2 × 5 cm silica gel column packed in hexane) eluting with hexane/CH_2Cl_2 (2:1) (20 mL) and hexane/CH_2Cl_2 (1:1) (30 mL) furnished $\mathbf{6}_{tBu}$ as a dark red solid (49 mg, 79%). Anal. Calcd (%) for $C_{66}H_{96}Ge_3N_6O_9Ru_3$ (M_W = 1638.54): C, 48.38; H, 5.91; N, 5.13. Found: C, 48.50; H, 6.00; N, 5.09. (+)-FAB MS: *m/z* 1639 $[M]^+$. IR (toluene, cm^{-1}): ν_{CO} 2020 (w), 1954 (vs), 1946 (vs), 1921 (vs). ^1H NMR (C_7D_8, 300.1 MHz, 293 K): δ 7.55 (m, 1 H, 1 C*H* of Ph), 7.11−6.86 (m, 4 H, 4 C*H* of Ph), 1.59 (s, 9 H, 3 *Me* of ^{t}Bu), 1.21 (s, 18 H, 6 *Me* of 3 ^{t}Bu). $^{13}C\{^1H\}$ NMR (C_7D_8, 75.5 MHz, 293 K): δ 215.9 (*C*Os), 169.2 (*N*CN), 134.5 (C_{ipso} of Ph), 130.9−127.3 (5 *C*H of Ph), 53.9 (2 *C* of 2 ^{t}Bu), 38.1 (*C* of ^{t}Bu), 32.5 (6 *Me* of 2 ^{t}Bu), 28.6 (3 *Me* of ^{t}Bu).

$[Ru_3(\mathbf{1}_{iPr})_3(CO)_9]$ ($\mathbf{6}_{iPr}$). A toluene solution of $\mathbf{1}_{iPr}$ (1.40 mL, 0.24 M, 0.336 mmol) was added to a solution of $[Ru_3(CO)_{12}]$ (50 mg, 0.080 mmol) in 8 mL of toluene, and the mixture was stirred at room temperature for 1 h. The initial orange color turned to dark orange. Purification by flash chromatography (2 × 3 cm silica gel column packed in hexane) eluting with CH_2Cl_2 (20 mL) furnished $\mathbf{6}_{iPr}$ as an orange solid (8 mg, 6%). Anal. Calcd for $C_{60}H_{84}Ge_3N_6O_9Ru_3$ (M_W = 1554.38): C, 46.36; H, 5.45; N, 5.41. Found: C, 46.56; H, 5.66; N, 5.40%. (+)-FAB MS: *m/z* = 1554 $[M]^+$. IR (toluene, cm^{-1}): ν_{CO} 2025 (w), 1962 (vs), 1955 (vs), 1925 (vs). ^1H NMR (C_6D_6, 300.1 MHz, 293 K): δ 6.99 (m, 5 H, 5 C*H* of Ph), 3.49 (m, 2 H, 2 C*H* of 2 ^{i}Pr), 1.58 (s, 9 H, 3 *Me* of ^{t}Bu), 1.31 (d, *J* = 6.6 Hz, 6 H, 2 *Me* of ^{i}Pr), (d, *J* = 6.6 Hz, 6 H, 2 *Me* of ^{i}Pr). The $^{13}C\{^1H\}$ NMR spectrum of this compound could not be obtained due to insufficient amount of sample.

$[Ru_2(\mu\text{-}\kappa^2\text{-}Ge,N\text{-}\mathbf{1}_{iPr})(CO)_7]$ ($\mathbf{7}_{iPr}$). A toluene solution of $\mathbf{1}_{iPr}$ (0.3 mL, 0.35 M, 0.105 mmol) was added to a toluene (8 mL) suspension of $[Ru_3(CO)_{12}]$ (50 mg, 0.080 mmol), and the mixture was stirred at 90 °C for 2 h. The initial orange color changed to dark red. Purification by flash chromatography (2 × 5 cm silica gel column packed in hexane) eluting with hexane (20 mL) and hexane/CH_2Cl_2 (1:1) (20 mL) afforded $\mathbf{7}_{iPr}$, which as isolated as a light red solid (52 mg, 59%). Anal. Calcd for $C_{24}H_{28}GeN_2O_7Ru_2$ (M_W = 731.24): C, 39.42; H, 3.86; N, 3.83. Found: C, 39.47; H, 3.89; N, 3.80%. (+)-FAB MS: *m/z* = 676 $[M - 2CO]^+$. IR (toluene, cm^{-1}): ν_{CO} 2081 (m), 2028 (vs), 2005 (s), 1999 (s), 1981 (m), 1950 (m). ^1H NMR (C_6D_6, 300.1 MHz, 293 K): δ = 6.91−6.85 (m, 4 H, 4 C*H* of Ph), 6.60 (m, 1 H, 1 C*H* of Ph), 3.71 (m, 1 H, C*H* of ^{i}Pr), 3.34 (m, 1 H, C*H* of ^{i}Pr), 1.46 (s, 9 H, 3 *Me* of ^{t}Bu), 1.15 (d, *J* = 6.6 Hz, 3 H, *Me* of ^{i}Pr), 0.93 (d, *J* = 6.9 Hz, 3 H, *Me* of ^{i}Pr), 0.80 (d, *J* = 6.5 Hz, 3 H, *Me* of ^{i}Pr), 0.65 (d, *J* = 7.0 Hz, 3 H, *Me* of ^{i}Pr). $^{13}C\{^1H\}$ NMR (C_6D_6, 75.5 MHz, 293 K): δ 202.7 (*C*Os), 202.6 (*C*Os), 202.4 (*C*Os), 201.3 (*C*Os), 169.8 (*N*CN), 137.1 (C_{ipso} of Ph), 128.6−126.5 (5 *C*H of Ph), 55.0 (*C*H of ^{i}Pr), 51.9 (*C*H of ^{i}Pr), 40.6 (*C* of ^{t}Bu), 30.6 (3 *Me* of ^{t}Bu), 26.1 (*Me* of ^{i}Pr), 24.1 (*Me* of ^{i}Pr), 22.9 (*Me* of ^{i}Pr), 22.2 (*Me* of ^{i}Pr).

X-ray Diffraction Analyses. Diffraction data were collected on Oxford Diffraction Xcalibur Onyx Nova ($\mathbf{3}_{iPr}$, $\mathbf{6}_{iPr}\cdot C_7H_8$, and $\mathbf{7}_{iPr}$; Cu Kα radiation) and Xcalibur Ruby Gemini ($\mathbf{4}_{tBu}$; Mo Kα radiation) single-crystal diffractometers. Empirical absorption corrections were applied using the SCALE3 ABSPACK algorithm as implemented in

DOI: 10.1021/acs.inorgchem.5b00084
Inorg. Chem. 2015, 54, 2983−2994

CrysAlisPro RED.[30] The structures were solved using SIR-97.[31] Isotropic and full matrix anisotropic least-squares refinements were performed using SHELXL.[32] All non-H atoms were refined anisotropically. The toluene solvent molecule and two of the isopropyl groups (C20 and C45 are their methyne carbon atoms) of $\mathbf{6}_{iPr}\cdot C_7H_8$ were found disordered over two positions in 66:34, 57:43, and 53:47 ratios, respectively. Restraints were applied on the thermal and geometrical parameters of the atoms involved in this positional disorder. All H atoms were set in calculated positions and refined riding on their parent atoms. The WINGX program system[33] was used throughout the structure determinations. A selection of crystal, measurement, and refinement data is given in Table S1 of the Supporting Information. CCDC deposition numbers: 1032651 ($\mathbf{3}_{iPr}$), 1032652 ($\mathbf{4}_{tBu}$), 1032653 ($\mathbf{6}_{iPr}\cdot C_7H_8$), and 1032654 ($\mathbf{7}_{iPr}$).

Computational Details. DFT calculations were performed using the wB97XD functional,[34] which includes the second generation of Grimme's dispersion interaction correction[35] as well as long-range interactions effects. This functional was chosen because it provided the best overall performance in a study that compared its efficiency in reproducing the X-ray diffraction molecular structures of $\mathbf{3}_{iPr}$, $\mathbf{4}_{tBu}$, $\mathbf{6}_{iPr}$, and $\mathbf{7}_{iPr}$ with those of the two popular density functionals B3LYP[36] and M06.[37] The wB97XD functional reproduces the local coordination geometry of transition metal compounds very well, and it also corrects the systematic overestimation of nonbonded distances seen for all the density functionals that do not include estimates of dispersion.[38] The LanL2DZ basis set,[39] with relativistic effective core potentials, was used for the Ru and Ge atoms. The basis set used for the remaining atoms was the 6-31G(d,p).[40] All stationary points were fully optimized in gas phase and confirmed as energy minima by analytical calculation of frequencies (all positive eigenvalues). The electronic energies of the optimized structures were used to calculate the zero-point corrected energies and the enthalpic and entropic contributions via vibrational frequency calculations. Solvation free energies were obtained from the gas-phase calculations using the self-consistent reaction field approximation to the standard continuum solvation model (CPCM).[41,42] Free energies of reactions (Table 3) were obtained using the Born−Haber thermodynamic cycle. All calculations were performed with the Gaussian09 package.[43] DFT-calculated atomic coordinates of all the DFT-optimized structures are given in the Supporting Information file (Tables S2−S12).

■ ASSOCIATED CONTENT

Supporting Information

Figures containing ^{1}H and ^{13}C NMR spectra, crystallographic data (including CIF files), and atomic coordinates of all the DFT-optimized structures. This material is available free of charge via the Internet at http://pubs.acs.org.

■ AUTHOR INFORMATION

Corresponding Authors

*E-mail: jac@uniovi.es. (J.A.C.)
*E-mail: pga@uniovi.es. (P.G.-A.)

Notes

The authors declare no competing financial interest.

■ ACKNOWLEDGMENTS

This work was supported by a European Union Marie Curie reintegration grant (No. FP7-2010-RG-268329) and by Spanish MINECO-FEDER research grants (Nos. CTQ2010-14933, MAT2013-40950-R, CTQ2013-40619-P, and RYC-2012-10491).

■ REFERENCES

(1) For a review on the reactivity of $[Ru_3(CO)_{12}]$ with triorganophosphines, see: Bruce, M. I. In *Comprehensive Organometallic Chemistry;* Wilkinson, G., Stone, F. G. A., Abel, E. W., Bruce, M. I., Eds.; Pergamon: Oxford, U.K., 1982; Vol. 4, pp 843−888.

(2) For a review on the reactivity of $[Ru_3(CO)_{12}]$ with NHCs, see: Cabeza, J. A.; García-Álvarez, P. *Chem. Soc. Rev.* **2011**, *40*, 5389−5405.

(3) (a) Piacenti, F.; Bianchi, M.; Benedetti, E.; Sbrana, G. *J. Inorg. Nucl. Chem.* **1967**, *29*, 1389−1391. (b) Candlin, J. P.; Shortland, A. C. *J. Organomet. Chem.* **1969**, *16*, 289−299. (c) Bennett, R. L.; Bruce, M. I.; Stone, F. G. A. *J. Organomet. Chem.* **1972**, *38*, 325−334. (d) Bruce, M. I.; Shaw, G.; Stone, F. G. A. *J. Chem. Soc., Dalton Trans.* **1972**, 2094−2099. (e) Poë, A. J.; Twigg, M. V. *J. Chem. Soc., Dalton Trans.* **1974**, 1860−1866. (f) Poë, A. J.; Twigg, M. V. *Inorg. Chem.* **1974**, *13*, 2982−2985. (g) Brodie, N. M. J.; Poë, A. J. *Inorg. Chem.* **1988**, *27*, 3156−3159.

(4) (a) Bruce, M. I.; Cole, M. L.; Fung, R. S. C.; Forsyth, C. M.; Hilder, M.; Junk, P. C.; Konstas, K. *Dalton Trans.* **2008**, 4118−4128. (b) Ellul, C. E.; Saker, O.; Mahon, M. F.; Apperley, D. C.; Whittlesey, M. K. *Organometallics* **2008**, *27*, 100−108. (c) Crittall, M. R.; Ellul, C. E.; Mahon, M. F.; Saker, O.; Whittlesey, M. K. *Dalton Trans.* **2008**, 4209−4211. (d) Ellul, C. E.; Mahon, M. F.; Saker, O.; Whittlesey, M. K. *Angew. Chem., Int. Ed.* **2007**, *46*, 6343−6345. (e) Cabeza, J. A.; del Río, I.; Miguel, D.; Pérez-Carreño, E.; Sánchez-Vega, M. G. *Organometallics* **2008**, *27*, 211−217. (f) Zhang, C.; Li, B.; Song, H.; Xu, S.; Wang, B. *Organometallics* **2011**, *30*, 3029−3036.

(5) See, for example: (a) Alper, H.; Amaratunga, S. *Tetrahedron Lett.* **1980**, *21*, 2603−2604. (b) Blum, Y.; Reshef, D.; Shvo, Y. *Tetrahedron Lett.* **1980**, *22*, 1541−1544. (c) Cenini, S.; Crotti, C.; Pizzotti, M.; Porta, F. *J. Org. Chem.* **1988**, *53*, 1243−1250. (d) Ragaini, F.; Cenini, S.; Tollari, S.; Tummolillo, G.; Beltrami, R. *Organometallics* **1999**, *18*, 928−942. (e) Ragaini, F.; Cenini, S. *Organometallics* **1999**, *18*, 4925−4933. (f) Tobisu, M.; Chatani, N.; Asaumi, T.; Amako, K.; Fukumoto, Y.; Ie, Y.; Murai, S. *J. Am. Chem. Soc.* **2000**, *122*, 12663−12674. (g) Pingen, D.; Müller, C.; Vogt, D. *Angew. Chem., Int. Ed.* **2010**, *49*, 8130−8133. (h) Wu, L.; Fleischer, I.; Jackstell, R.; Profir, I.; Franke, R.; Beller, M. *J. Am. Chem. Soc.* **2013**, *135*, 14306−14312.

(6) Lee, V. Y.; Sekiguchi, A. *Organometallic Compounds of Low Coordinate Si, Ge, Sn and Pb: From Phantom Species to Stable Compounds;* Wiley-VCH: Chichester, U.K., 2010.

(7) For recent reviews on the synthesis and general chemistry of HTs, see: (a) Izod, K. *Coord. Chem. Rev.* **2013**, *257*, 924−945. (b) Xiong, Y.; Yao, S.; Driess, M. *Angew. Chem., Int. Ed.* **2013**, *52*, 4302−4311. (c) Mandal, S. K.; Roesky, H. W. *Acc. Chem. Res.* **2012**, *45*, 298−307. (d) Yao, S.; Xiong, Y.; Driess, M. *Organometallics* **2011**, *30*, 1748−1767. (e) Mizuhata, Y.; Sasamori, T.; Tokitoh, N. *Chem. Rev.* **2009**, *109*, 3479−3511.

(8) For recent reviews on the derivative chemistry of HTs, including TM complexes, see: (a) Blom, B.; Stoelzel, M.; Driess, M. *Chem.—Eur. J.* **2013**, *19*, 40−62. (b) Ghadwal, R. S.; Azhakar, R.; Roesky, H. W. *Acc. Chem. Res.* **2013**, *46*, 444−456. (c) Roesky, H. W. *J. Organomet. Chem.* **2013**, *730*, 57−62. (d) Asay, M.; Jones, C.; Driess, M. *Chem. Rev.* **2011**, *111*, 354−396. (e) Mandal, S. K.; Roesky, H. W. *Chem. Commun.* **2010**, *46*, 6016−6041. (f) Kira, M. *Chem. Commun.* **2010**, *46*, 2893−2903. (g) Nagendran, S.; Roesky, H. W. *Organometallics* **2008**, *27*, 457−492. (h) Zabula, A. V.; Hahn, F. E. *Eur. J. Inorg. Chem.* **2008**, 5165−5179. (i) Leung, W.-P.; Kan, K.-W.; Chong, K.-H. *Coord. Chem. Rev.* **2007**, *251*, 2253−2265. (j) Waterman, R.; Hayes, P. G.; Tilley, T. D. *Acc. Chem. Res.* **2007**, *40*, 712−719.

(9) For TM complexes containing amidinate-tetrylene ligands, see: (a) Gallego, D.; Brück, A.; Irran, E.; Meier, F.; Kaupp, M.; Driess, M.; Hartwig, J. F. *J. Am. Chem. Soc.* **2013**, *135*, 15617−15626. (b) Blom, B.; Enthaler, S.; Inoue, S.; Irran, E.; Driess, M. *J. Am. Chem. Soc.* **2013**, *135*, 6703−6713. (c) Someya, C. I.; Haberberger, M.; Wang, W.; Enthaler, S.; Inoue, S. *Chem. Lett.* **2013**, *42*, 286−288. (d) Wang, W.; Inoue, S.; Enthaler, S.; Driess, M. *Angew. Chem., Int. Ed.* **2012**, *51*, 6167−6171. (e) Brück, A.; Gallego, D.; Wang, W.; Irran, E.; Driess, M.; Hartwig, J. F. *Angew. Chem., Int. Ed.* **2012**, *51*, 11478−11482. (f) Blom, B.; Driess, M.; Gallego, D.; Inoue, S. *Chem.—Eur. J.* **2012**, *18*, 13355−13360. (g) Azhakar, R.; Ghadwal, R. S.; Roesky, H. W.; Hey, J.; Stalke, D. *Chem. Asian. J.* **2012**, *7*, 528−533. (h) Azhakar, R.; Ghadwal, R. S.; Roesky, H. W.; Wolf, H.; Stalke, D. *J. Am. Chem. Soc.* **2012**, *134*, 2423−2428. (i) Junold, K.; Baus, J. A.; Burschka, C.; Tacke, R. *Angew. Chem., Int. Ed.* **2012**, *51*, 7020−7023. (j) Azhakar, R.;

DOI: 10.1021/acs.inorgchem.5b00084
Inorg. Chem. 2015, 54, 2983−2994

Roesky, H. W.; Holstein, J. J.; Dittrich, B. *Dalton. Trans.* **2012**, *41*, 12096−12100. (k) Wang, W.; Inoue, S.; Irran, E.; Driess, M. *Angew. Chem., Int. Ed.* **2012**, *51*, 3691−3694. (l) Azhakar, R.; Sarish, S. P.; Roesky, H. W.; Hey, J.; Stalke, D. *Inorg. Chem.* **2011**, *50*, 5039−5043. (m) Tavčar, G.; Sen, S. S.; Azhakar, R.; Thorn, A.; Roesky, H. W. *Inorg. Chem.* **2010**, *49*, 10199−10202. (n) Wang, W.; Inoue, S.; Yao, S.; Driess, M. *J. Am. Chem. Soc.* **2010**, *132*, 15890−1589. (o) Matioszek, D.; Katir, N.; Saffon, N.; Castel, A. *Organometallics* **2010**, *29*, 3039−3046. (p) Sen, S. S.; Kritzler-Kosch, M. P.; Nagendran, S.; Roesky, H. W.; Beck, T.; Pal, A.; Herbst-Irmer, R. *Eur. J. Inorg. Chem.* **2010**, 5304−5311. (q) Yang, W.; Fu, H.; Wang, H.; Chen, M.; Ding, Y.; Roesky, H. W.; Jana, A. *Inorg. Chem.* **2009**, *48*, 5058−5060. (r) Jones, C.; Rose, R. P.; Stasch, A. *Dalton Trans.* **2008**, 2871−2878. (s) Junold, K.; Baus, J. A.; Burschka, C.; Vent-Schmidt, T.; Riedel, S.; Tacke, R. *Inorg. Chem.* **2013**, *52*, 11593−11599. (t) Azhakar, R.; Ghadwal, R. S.; Roesky, H. W.; Hey, J.; Krause, L.; Stalke, D. *Dalton. Trans.* **2013**, *42*, 10277−10281. (u) Tan, G.; Blom, B.; Gallego, G.; Driess, M. *Organometallics* **2014**, *33*, 363−369. (v) Sen, S. S.; Kratzer, D.; Stern, D.; Roesky, H. W.; Stalke, D. *Inorg. Chem.* **2010**, *49*, 5786−5788. (w) Breit, N. C.; Szilvási, T.; Suzuki, T.; Gallego, D.; Inoue, S. *J. Am. Chem. Soc.* **2013**, *135*, 17958−17968.

(10) For a recent review on N-heterocyclic silylene complexes in catalysis, see: Blom, B.; Gallego, D.; Driess, M. *Inorg. Chem. Front.* **2014**, *1*, 134−148.

(11) (a) Cabeza, J. A.; García-Álvarez, P.; Pérez-Carreño, E.; Polo, D. *Inorg. Chem.* **2014**, *53*, 8735−8741. (b) Álvarez-Rodríguez, L.; Cabeza, J. A.; García-Álvarez, P.; Polo, D. *Organometallics* **2013**, *32*, 3557−3561. (c) Cabeza, J. A.; Fernández-Colinas, J. M.; García-Álvarez, P.; Polo, D. *Inorg. Chem.* **2012**, *51*, 3896−3903. (d) Cabeza, J. A.; García-Álvarez, P.; Polo, D. *Inorg. Chem.* **2012**, *51*, 2569−2576. (e) Cabeza, J. A.; García-Álvarez, P.; Polo, D. *Inorg. Chem.* **2011**, *50*, 6195−6199.

(12) Cabeza, J. A.; García-Álvarez, P.; Polo, D. *Dalton. Trans.* **2013**, *42*, 1329−1332.

(13) Cabeza, J. A.; Fernández-Colinas, J. M.; García-Álvarez, P.; Polo, D. *RSC Adv.* **2014**, *4*, 31503−31506.

(14) Cabeza, J. A.; García-Álvarez, P.; Pérez-Carreño, E.; Polo, D. *Chem.—Eur. J.* **2014**, *20*, 8654−8663.

(15) A related chelating κ^2-*N*,*Si*-imine-silylene behavior has been recently observed in carbonyl group-6 TM complexes for guanidinate-silylene ligands containing isopropyl groups on the coordinated N atoms: Mück, F. M.; Kloss, D.; Baus, J. A.; Burschka, C.; Tacke, R. *Chem.—Eur. J.* **2014**, *20*, 9620−9626.

(16) Chen, L.; Poë, A. J. *Inorg. Chem.* **1989**, *28*, 3641−3647.

(17) Jazzar, R. F. R.; Bhatia, P. H.; Mahon, M. F.; Whittlesey, M. K. *Organometallics* **2003**, *22*, 670−683.

(18) Burling, S.; Kociok-Köhn, G.; Mahon, M. F.; Whittlesey, M. K.; Williams, J. M. J. *Organometallics* **2005**, *24*, 5868−5878.

(19) Davies, C. J. E.; Lowe, J. P.; Mahon, M. F.; Poulten, R. C.; Whittlesey, M. K. *Organometallics* **2013**, *32*, 4927−4937.

(20) Bruce, M. I.; Matisons, J. G.; Nicholson, B. K. *J. Organomet. Chem.* **1983**, *247*, 321−343.

(21) (a) Mayr, A.; Lin, Y. C.; Boag, N. M.; Kaesz, H. D. *Inorg. Chem.* **1982**, *21*, 1704−1706. (b) Jensen, C. M.; Lynch, T. J.; Knobler, C. B.; Kaesz, H. D. *J. Am. Chem. Soc.* **1982**, *104*, 4679−4680. (c) Lavigne, G.; Kaesz, H. D. *J. Am. Chem. Soc.* **1984**, *106*, 4647−4648.

(22) (a) Morris, D. E.; Basolo, F. *J. Am. Chem. Soc.* **1968**, *90*, 2531−2535. (b) Basolo, F. *Inorg. Chim. Acta* **1981**, *50*, 65−70.

(23) Liu, Y.; Ganguly, R.; Huynh, H. V.; Leong, W. K. *Angew. Chem., Int. Ed.* **2013**, *52*, 12110−12113.

(24) Connor, J. A. *Top. Curr. Chem.* **1977**, *71*, 71−110.

(25) Dyson, P. J.; McIndoe, J. S. *Transition Metal Carbonyl Cluster Chemistry;* Gordon and Breach Science Publishers: Amsterdam, 2000; p 94.

(26) Malik, S. K.; Poë, A. J. *Inorg. Chem.* **1978**, *17*, 1484−1488.

(27) (a) Johnson, B. F. G.; Lewis, J.; Twigg, M. V. *J. Organomet. Chem.* **1974**, *67*, C75−C76. (b) Forebs, E. J.; Goodhand, N.; Jones, D. L.; Hamor, T. A. *J. Organomet. Chem.* **1979**, *182*, 143−154.

(28) See, for example: (a) Cabeza, J. A.; del Río, I.; Miguel, D.; Pérez-Carreño, E.; Sánchez-Vega, M. G. *Dalton Trans.* **2008**, 1937−1942. (b) Cabeza, J. A.; Pérez-Carreño, E. *Organometallics* **2008**, *27*, 4697−4702. (c) Cabeza, J. A.; del Río, I.; Miguel, D.; Sánchez-Vega, M. G. *Angew. Chem., Int. Ed.* **2008**, *47*, 1920−1922. (d) Cabeza, J. A.; del Río, I.; Pérez-Carreño, E.; Sánchez-Vega, M. G.; Vázquez-García, D. *Angew. Chem., Int. Ed.* **2009**, *48*, 555−558.

(29) Nagendran, S.; Sen, S. S.; Roesky, H. W.; Koley, D.; Brubmüller, H.; Pal, A.; Herbst-Irmer, R. *Organometallics* **2008**, *27*, 5459−5463.

(30) *CrysAlisPro RED,* version 1.171.34.36; Oxford Diffraction Ltd.: Oxford, U.K., 2010.

(31) Altomare, A.; Burla, M. C.; Camalli, M.; Cascarano, G. L.; Giacovazzo, C.; Guagliardi, A.; Moliterni, A. G. C.; Polidori, G.; Spagna, R. *J. Appl. Crystallogr.* **1999**, *32*, 115−119.

(32) Sheldrick, G. M. *Acta Crystallogr.* **2008**, *A64*, 112−122.

(33) Farrugia, L. J. *J. Appl. Crystallogr.* **1999**, *32*, 837−838.

(34) Chai, J.-D.; Head-Gordon, M. *Phys. Chem. Chem. Phys.* **2008**, *10*, 6615−6620.

(35) (a) Ehrlich, S.; Moellmann, J.; Grimme, S. *Acc. Chem. Res.* **2013**, *46*, 916−926. (b) Grimme, S. *Comp. Mol. Sci.* **2011**, *1*, 211−228. (c) Schwabe, T.; Grimme, S. *Acc. Chem. Res.* **2008**, *41*, 569−579.

(36) (a) Becke, A. D. *J. Chem. Phys.* **1993**, *98*, 5648−5652. (b) Lee, C.; Yang, W.; Parr, R. G. *Phys. Rev. B* **1988**, *37*, 785−789.

(37) Zhao, Y.; Truhlar, D. G. *Theor. Chem. Acc.* **2008**, *120*, 215−241.

(38) Minenkov, Y.; Singstad, Å.; Occhipinti, G.; Jensen, V. R. *Dalton Trans.* **2012**, *41*, 5526−5541.

(39) Hay, P. J.; Wadt, W. R. J. *Chem. Phys.* **1985**, *82*, 299−310.

(40) Hariharan, P. C.; Pople, J. A. *Theor. Chim. Acta* **1973**, *28*, 213−222.

(41) Barone, V.; Cossi, M. *J. Phys. Chem. A* **1998**, *102*, 1995−2001.

(42) Cossi, M.; Rega, N.; Scalmani, G.; Barone, V. *J. Comput. Chem.* **2003**, *24*, 669−681.

(43) Frisch, M. J.; Trucks, G. W.; Schlegel, H. B.; Scuseria, G. E.; Robb, M. A.; Cheeseman, J. R.; Scalmani, G.; Barone, V.; Mennucci, B.; Petersson, G. A.; Nakatsuji, H.; Caricato, M.; Li, X.; Hratchian, H. P.; Izmaylov, A. F.; Bloino, J.; Zheng, G.; Sonnenberg, J. L.; Hada, M.; Ehara, M.; Toyota, K.; Fukuda, R.; Hasegawa, J.; Ishida, M.; Nakajima, T.; Honda, Y.; Kitao, O.; Nakai, H.; Vreven, T.; Montgomery, J. A., Jr.; Peralta, J. E.; Ogliaro, F.; Bearpark, M.; Heyd, J. J.; Brothers, E.; Kudin, K. N.; Staroverov, V. N.; Keith. T.; Kobayashi, R.; Normand, J.; Raghavachari, K.; Rendell, A.; Burant, J. C.; Iyengar, S. S.; Tomasi, J.; Cossi, M.; Rega, N.; Millam, N. J.; Klene, M.; Knox, J. E.; Cross, J. B.; Bakken, V.; Adamo, C.; Jaramillo, J.; Gomperts, R.; Stratmann, R. E.; Yazyev, O.; Austin, A. J.; Cammi, R.; Pomelli, C.; Ochterski, J. W.; Martin, R. L.; Morokuma, K.; Zakrzewski, V. G.; Voth, G. A.; Salvador, P.; Dannenberg, J. J.; Dapprich, S.; Daniels, A. D.; Farkas, Ö.; Foresman, J. B.; Ortiz, J. V.; Cioslowski, J.; Fox, D. J. *Gaussian 09,* revision B.01; Gaussian, Inc.: Wallingford, CT, 2010.

DOI: 10.1021/acs.inorgchem.5b00084
Inorg. Chem. 2015, 54, 2983−2994